DELINEATION OF KEY REGULATORY ELEMENTS IDENTIFIES POINTS OF VULNERABILITY IN THE MITOGEN-ACTIVATED SIGNALING NETWORK

SUPPLEMENTARY MATERIALS

List of contents

Supplementary Figures with legends

Supplementary Tables

Figure S1

A

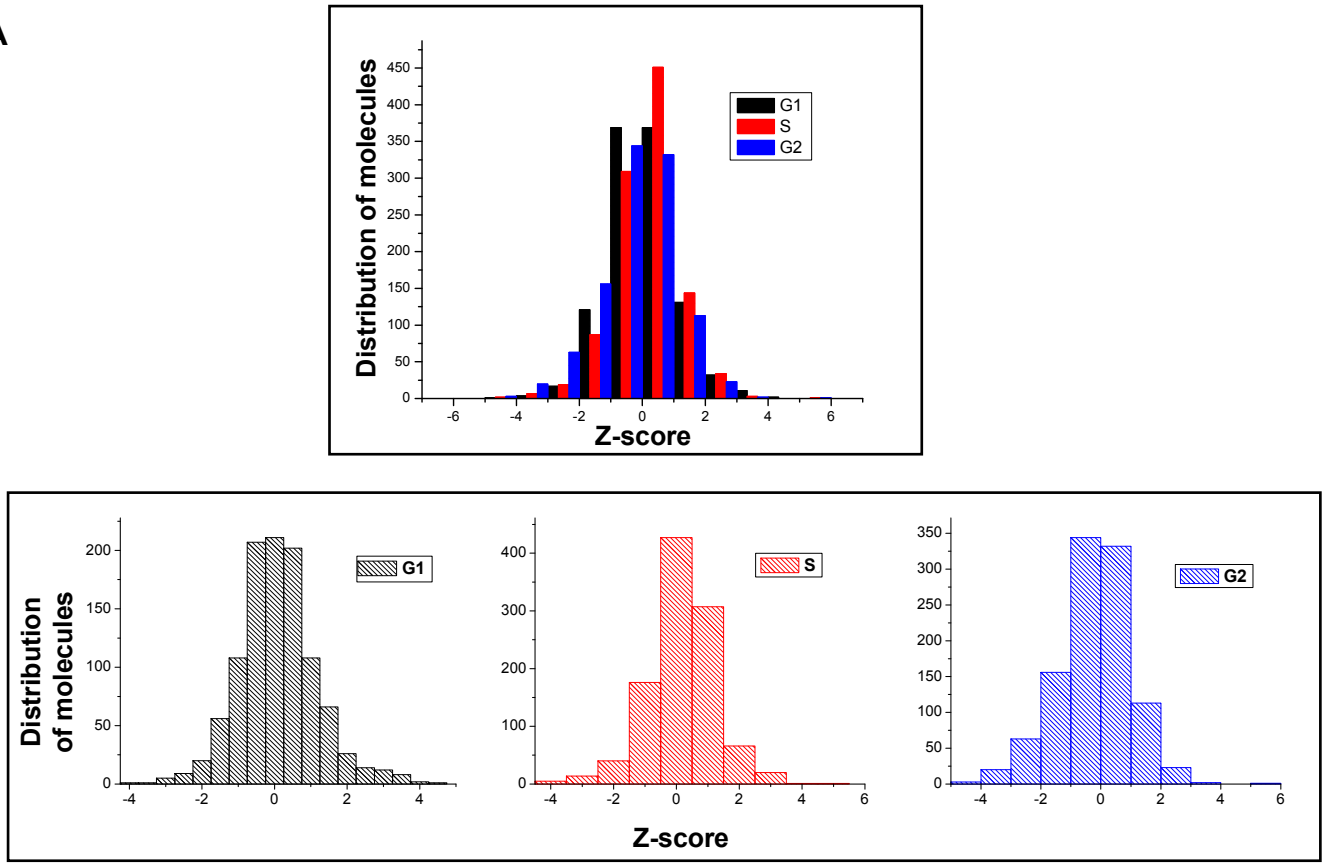
Distribution of molecules
Z-score
G1
S
G2
Distribution of molecules
Z-score
G1
S
G2

B

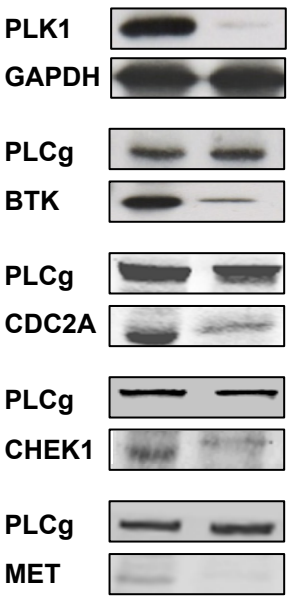
PLK1
GAPDH
PLCg
BTK
PLCg
CDC2A
PLCg
CHEK1
PLCg
MET

Distribution profiles of complete primary screen and western blots showing knockdown efficiency.

Plotted in **panel A** are the mean z-scores of the replicates for the entire screen with siRNA targeting kinases and phosphatases. The graph shows the distribution of the data points for all the molecules targeted. The normal nature of the distribution curve, with minimal skewness, confirms the robustness of the screen.

Panel B shows the effect of siRNA knockdown of 5 targets at 96 hours post transfection. siRNAs targeting BTK and PLK1 were used for screen standardizations. The reductions in protein levels were monitored at 24, 36, 48, 72 and 96 hours post transfection. At each of these time points cells were harvested, lysed and the levels of the respective proteins in the cytoplasm detected by Western blot analysis. Silencing of select proteins, which includes 3 validated screen hits (CHEK1, MET and CDC2A) at 96 hours after transfection is shown here. Here either GAPDH (for PLK1), or PLCg (for the remaining molecules) were also probed in parallel to serve as the loading control. The antibodies were obtained from Cell Signaling Technology. (Also refer Figure 1).

Figure S2

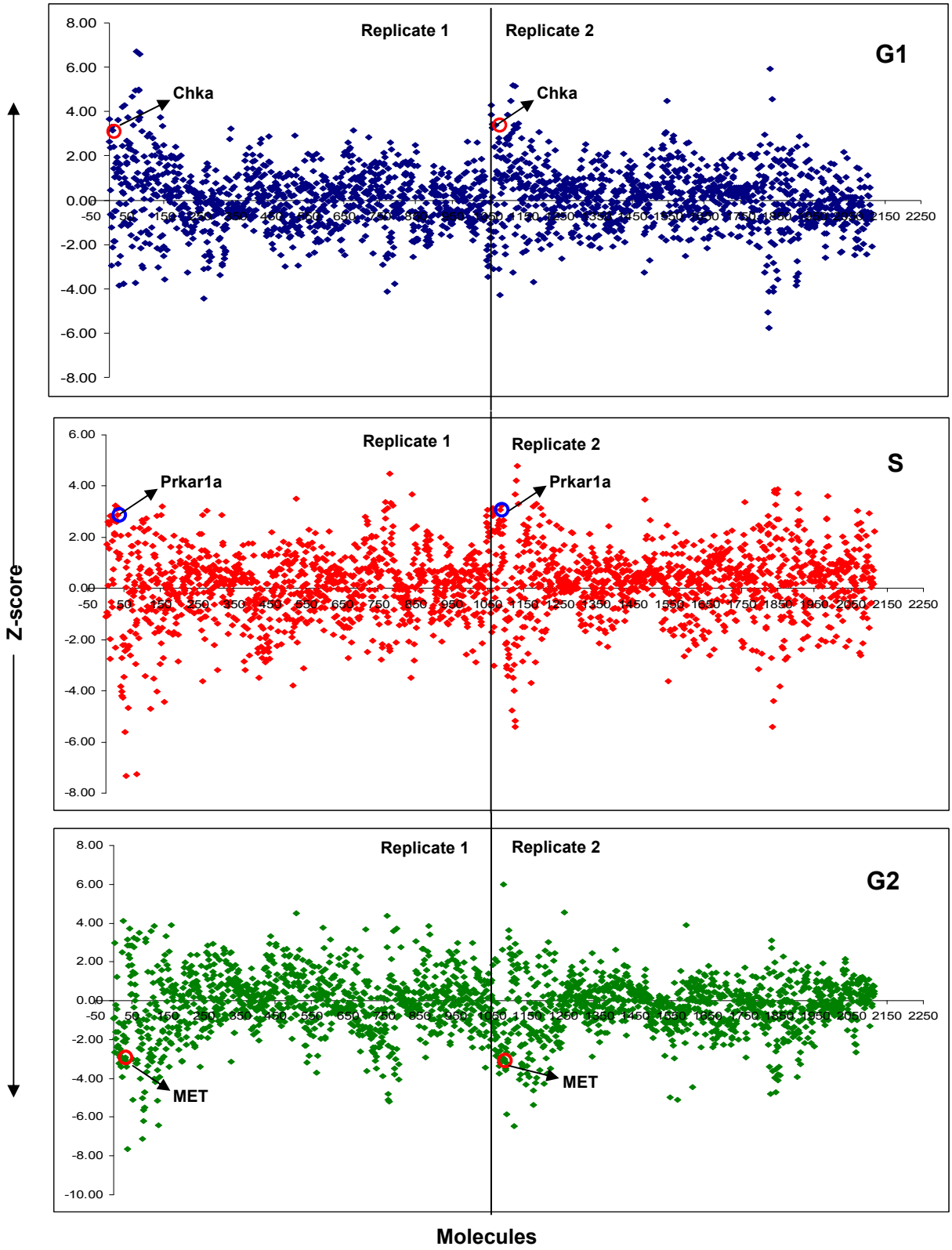

Scatter plot of z-scores to verify reproducibility of the primary siRNA screen

Shown are the scatter plots for the two individual replicate z-scores for the three different phases. (Refer Figure 1)

Figure S3

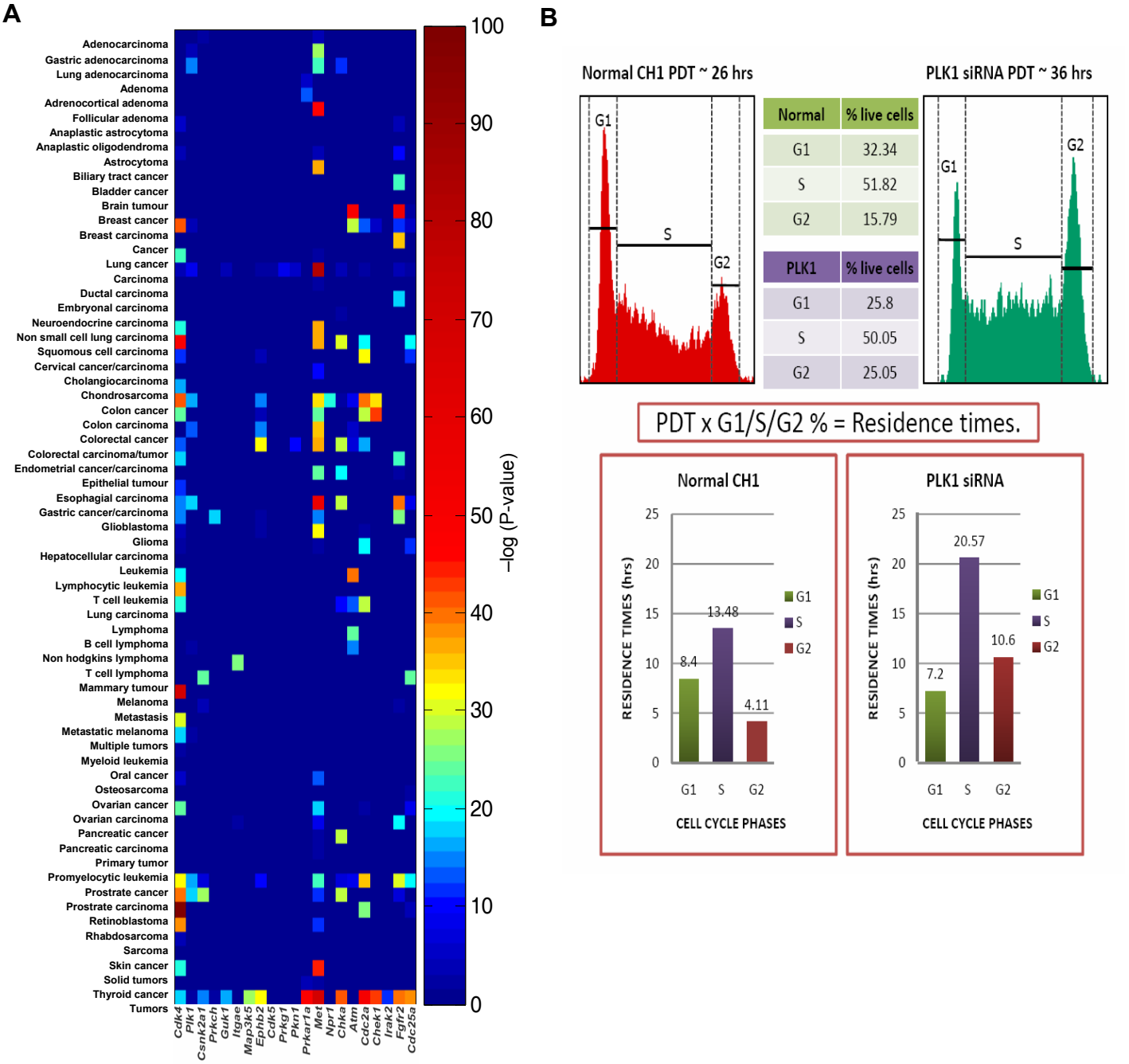

Functional relevance of the identified targets and Calculation of residence time from PDT and cell cycle distribution

Panel A depicts the gene-disease relationship score (indicated by the color bar) of our hits with various forms of cancer. These scores were obtained as –log (P-value) from Novoseek gene-disease database.

Panel B shows the schematic to explain the method followed to calculate RT for CH1 cells after targeted siRNA mediated perturbation of screen hits. The approach is illustrated by taking the case of PLK1 as a typical example. (Refer Figure 1C and 1D)

Figure S4

A

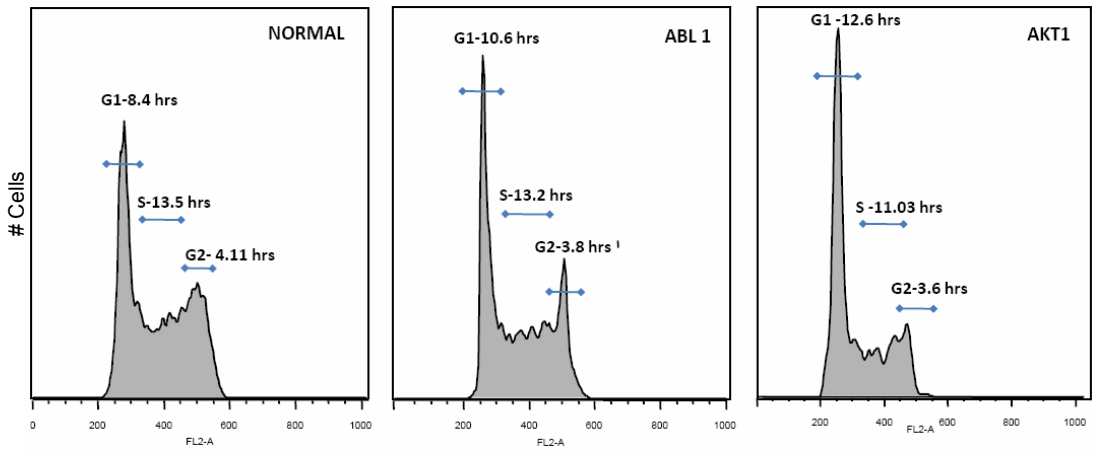

B

	siRNA sequence 1	siRNA sequence 2	siRNA sequence 3	siRNA sequence 4
BRCA1	GAGCAGCCCUUCACAAAUA	GGAGGAAAGUGGAUAGUUA	GUAGUAAUCUCCAGAAAGA	GAAUGCAGCUUACAAAUGG
ESR1	GGACUUGAAUCUCCAUGAU	UCAAGUCGGUUCCGCAUGA	GAAAGGCGGCAUACGGAAA	GACAAUCGACGCCAGAAUG
PTK2B	GAACCCACCUGGAUUAUCA	GAACAUGGCUGAUCUCAUA	GGACGAAGACUAUUACAAA	GAACAAGCUUGGCCAGUUG
SKP2	CCGGUGCUAUGAUAUAAUA	CGAACUCAGUGAUAAAUGU	CGACUUAAGUGACAGUAUC	GGAAACGAGUCAAGGGCAA
JUN	GAACAGGUGGCACAGCUUA	GAAACGACCUUCUACGACG	CCAAGAACGUGACCGACGA	GCCAAGAACUCGGACCUUC
RB1	GGAGUUUGAUUCCAUUAUA	GCAUAUCUCCGACUAAAUA	UCGAAGCCCUUACAAGUUU	UGCGUUAUCUACUGAAAUA
E2F1	CCACGAGGCCCUUGACUAU	UACAAGCUGUGGAUUCUUC	GGAGGGUGAGGGCAUUAGA	GCAAACAAGGCCCCAUUGA

Panel A shows the histograms obtained from a cell cycle analysis of CH1 cells at 48 hours post treatment with 0.5 x IC50 of ABL1 and AKT1 inhibitor (i.e Imatinib mesylate and LY294002). The respective RTs of the G1, S and G2 phases are indicated. (Figure 5A).

Panel B lists the siRNA sequences employed for silencing of the high stress and betweeness targets shown in Figure 5B.

Figure S5

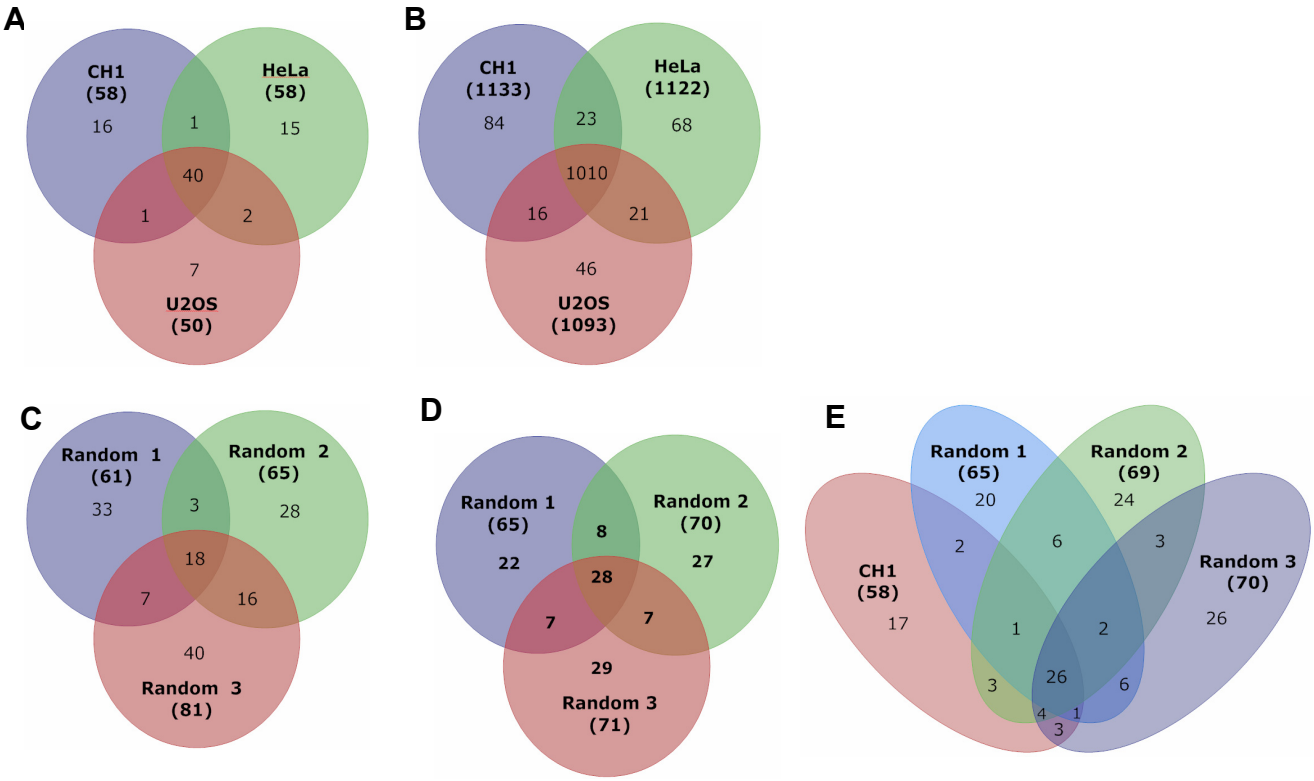

Panel A shows the Venn diagram comparing the overlap of IMP nodes identified from the three different screens.

Panel B shows the Venn diagram comparing the overlap of nodes from the IMP node networks of the three different screens.

Panel C is the comparison between IMP nodes identified from three sets of randomly sampled source-target pairs. A very poor overlap can be observed here.

Panel D is the comparison between IMP nodes identified from three sets of randomly sampled sources but retaining the target nodes to assess target biasness in IMP nodes selection. Again a very poor overlap can be observed here.

Panel E is the comparison between IMP nodes identified from three sets of randomly sampled sources and the IMP nodes identified from our study in CH1. A very poor overlap can be observed here when compared to the overlap observed between U2OS and HeLa cells.

Figure S6

A

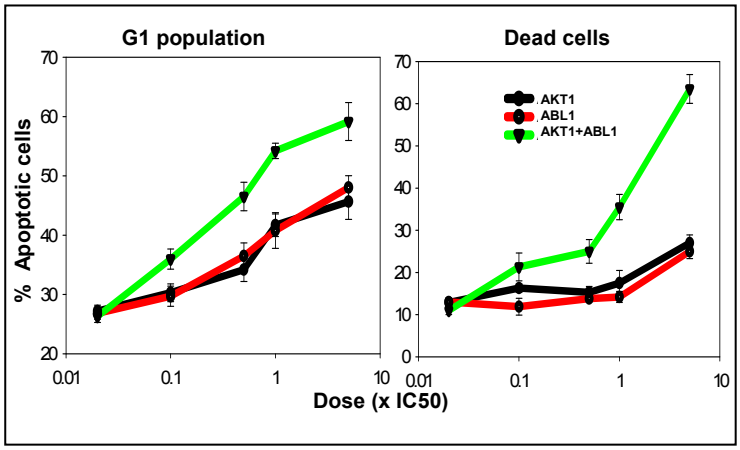

B

		LIST OF HUMAN CELL LINES USED
	CELL LINE	DESCRIPTION
1	A549	Human alveolar epithelial cell line
2	AW8507	Human buccal cancer cell lines
3	MCF7	Human breast epithelial adenocarcinoma
4	HEK293	Human embryonic kidney
5	HELA	Human epithelial carcinoma cell line
6	HEPG2	Human hepatocellular liver carcinoma cell line
7	HL-60	Human promyelocytic leukemia cells
8	HUH7	Human hepatoma cell line
9	JURKAT	Human T cell lymphoblast-like cell line
10	NAMALWA	Human burkitts lymphoma
11	RAJI	Human burkitts lymphoma
12	THP1	Human acute monocytic leukemia cell line
13	U20S	Human osteosarcoma expressing wt p53 and Rb
14	U937	Human leukemic monocyte lymphoma cell line

C

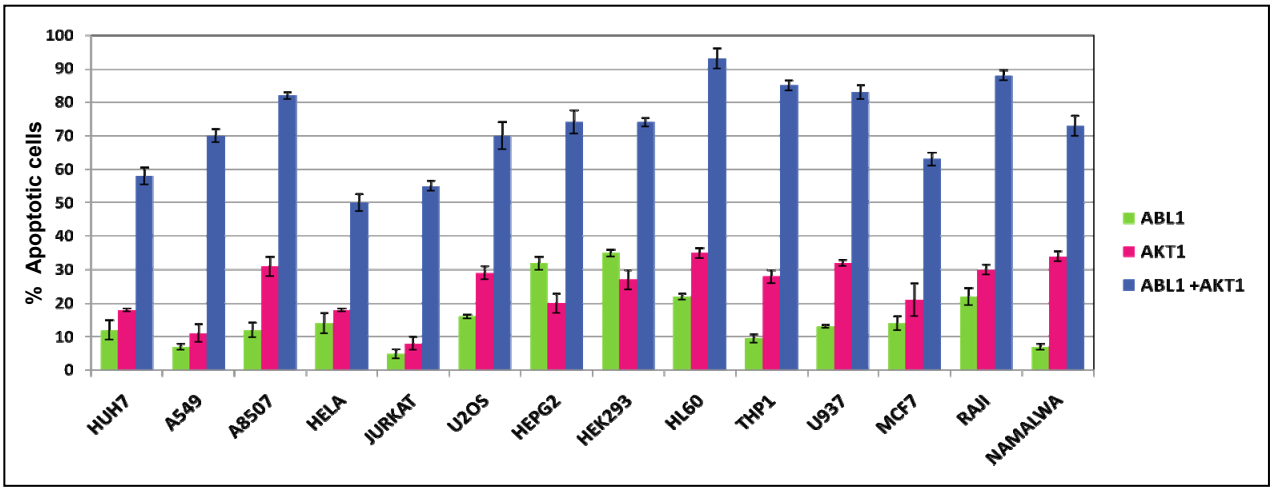

D

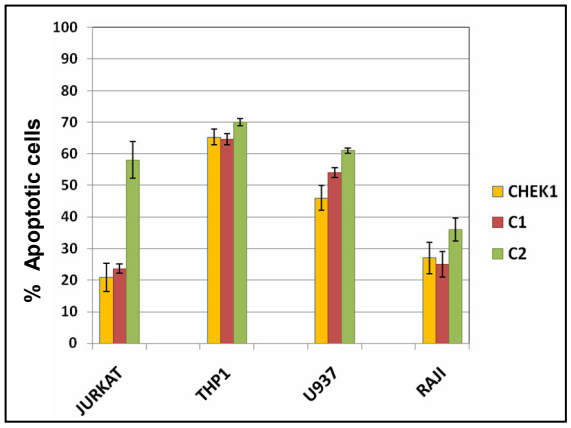

E

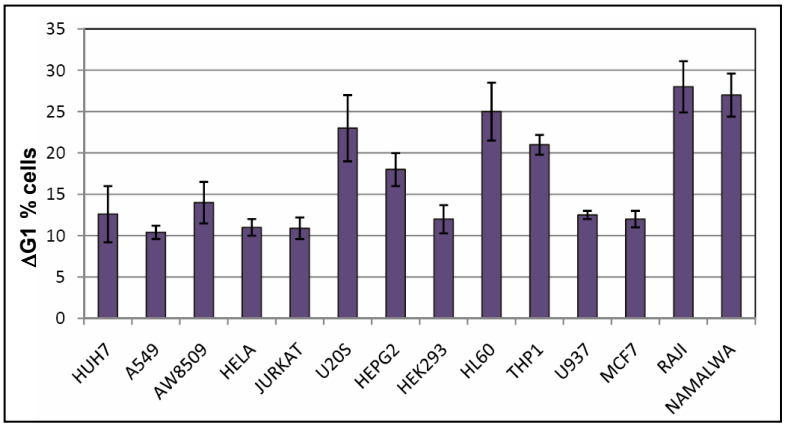

Panel A depicts the dose-response profile for increase in G1 population, and increase in apoptotic cells in CH1 cells treated with pharmacological inhibitors of ABL1, AKT1 and the combination of the respective doses. Doses for each inhibitor used were in multiples of their corresponding IC50 values as indicated. Values (mean ± S.D. of three experiments) are expressed as the percent of cells obtained at 48h post treatment. (Also refer Figure 5).

Panel B lists and describes all the human cell lines used in this study.

In **Panel C**, the effect of inhibition of ABL1, AKT1 and their combination (at concentrations corresponding to 5 times their respective IC50 values) on inducing apoptosis of fourteen different human cancer cell lines is shown. Here, the cells were treated with a single addition of the inhibitor or inhibitor combination, and the frequency of apoptotic cells was determined 48h later. In all cases, results are the mean (± S.D.) of three experiments.

In **Panel D**, cells of the indicated cancer cell lines were treated with inhibitors against either the indicated kinase, or the kinase combinations and the consequent effect on cellular apoptosis was determined 48 hours later. The concentration of the relevant inhibitor employed was five-fold greater than its corresponding IC50 value in all cases and results are the mean (± S.D.) of three experiments. The protocol followed was similar to panel C. As is evident, with the exception of Jurkat cells, apoptosis resulted from the dominant effects of CHEK1 inhibition in all cases (Refer Figure 7).

Panel E depicts the increase in G1 population observed in the fourteen different human cancer cell lines following treatment with inhibitors of both ABL1 and AKT1 (at concentration corresponding to their IC50 values). Values (mean ± S.D., n=3) are those obtained at 24 h post-treatment and are expressed as increase in the percent of cells in the G1 phase, relative to that in the absence of any inhibitor (i.e. vehicle only).

Table S3

Classification of hits based on RT affecting the cell cycle phases

		Observed Phenotype (Based on increase in RT)	Pubmed IDs for Cell Cycle role known			Role in cell proliferation	Total No. of GO terms	GO Involved Cell Cycle or Proliferation	Ratio	Residence Time (Hours)			Population Doubling time (Hours)	Std. Dev (± hours)			
			G1 and G1/S	S	G2					G1	S	G2	PDT	G1 (SD)	S (SD)	G2 (SD)	PDT (SD)
1	***Atm***	G1	7923116	11544175:8843193	--	--	13	5	0.4	10.2	11.5	3	23.9	0.5	0.7	0.2	1.5
2	***Chek1***	G1	11544175	11544175	11544175	--	4	3	0.8	12.2	15.2	3.1	29.5	0.8	1.1	0.3	2.3
3	***Fgfr2***	G1	--	--	--	10572038:15199177	55	3	0.1	11.7	10	3.8	25.6	1.6	1.7	0.6	3.9
4	***Irak2***	G1	--	--	--	--	3	0	0.0	10.7	11	3.8	26.5	1.1	1.3	0.5	2.9
5	***Lek1***	G1	14555653	--	--	--	14	4	0.3	13.9	14.2	3.8	31.4	1	1.2	0.3	2.6
6	***Mast2***	G1	--	--	--	--	3	0	0.0	14.7	13.2	2.8	32.8	1.4	1.4	0.4	3.2
7	***Pkig***	G1	--	--	--	--	2	0	0.0	9.6	13	4.1	25.8	0.8	1	0.4	2.2
8	***Pkn1***	G1	---	---	---	--	4	0	0.0	10.1	13.4	3.1	26.3	0.7	1.1	0.4	2.2
9	***Plk2***	G1	12972611	--	--	12972611	2	1	0.5	14.6	14.3	3.9	31.8	1	1.3	0.3	2.6
10	***Ripk3***	G1	--	--	--	10358032	4	2	0.5	10.5	13.5	2.2	26.1	0.5	0.7	0.2	1.4
11	***Tex14***	G1	--	--	--	--	1	0	0.0	11	14.8	1.9	27.5	1.6	2.2	0.5	4.2
12	***Vrk2***	G1	18286197		--	--	1	0	0.0	12.1	11.9	3.5	27.5	1.3	1.4	0.6	3.3
13	***Cdk4***	G1 and G2	19013283	---	16476733:10318807	---	4	2	0.5	8.7	12.7	4.8	26.4	0.6	0.9	0.3	1.8
14	***Cdc25a***	G1 and S	14681206:10454565	10454565:10995786	19192479	--	2	2	1.0	11	16.9	3.2	30.5	1	1.5	0.4	2.9
15	***Cdc2a***	G1 and S	17700700	17635936	19570916:19013283	--	3	3	1.0	14.9	14.9	3.4	32	0.9	1.2	0.3	2.4
16	***Cdk5***	G1 and S	8302605:1358458	---	---	--	6	2	0.3	11.5	19.5	3.3	33.6	0.8	1.2	0.3	2.3
17	***Chka***	G1 and S	18296102	---	---	--	1	0	0.0	17.7	17	3.1	37.8	1.4	1.7	0.4	3.5
18	***Dusp12***	G1 and S	--	--	--	16274472	4	0	0.0	10.3	20.2	3.9	34.4	0.7	1.3	0.3	2.4
19	***Map3k5***	G1 and S	--	---	---	15210709	1	0	0.0	11.9	25.4	3.4	41.4	1.3	2.3	0.5	4.1
20	***Map4k1***	G1 and S	14981547	15634691	--	--	3	0	0.0	9.8	14.9	2.8	28.1	0.9	1.4	0.4	2.7
21	***Met***	G1 and S	15064724	---	---	--	12	0	0.0	14	16.4	2.6	33.5	1.7	2.1	0.6	4.4
22	***Npr1***	G1 and S	--	--	--	--	3	0	0.0	9.4	14	3.1	27	0.8	1.3	0.4	2.6
23	***Prkar1a***	G1 and S	---	---	---	16569736	6	2	0.3	9.4	16.2	6.2	29.9	0.8	1.3	0.7	2.9
24	***Slk***	G1 and S	--	--	16236704	---	5	1	0.2	10.4	24	3.1	37.5	0.3	0.5	0.1	0.9
25	***Srms***	G1 and S	--	--	--	--	1	0	0.0	10.9	16.7	1.2	28.6	1.8	2.6	0.4	4.9
26	***Taok2***	G1 and S	--	--	--	10660600	1	0	0.0	13.6	17.1	1.4	31.8	1.4	1.7	0.3	3.4
27	***Trpm7***	G1 and S	19515901	---	---	18590694:19515901	1	0	0.0	11	16.2	2.1	29.2	1.3	1.8	0.5	3.7
28	***Tssk5***	G1 and S	--	--	--	--	1	0	0.0	9.8	15.2	1.8	26.6	1.4	2.1	0.4	3.9
29	***Csnk2a1***	G2	12396231	---	12396231	---	2	0	0.0	6.1	12.7	7.6	26.1	0.9	1.4	0.8	3.1
30	***Prkch***	G2	16434969	---		8454583:8336936: 9310352	1	0	0.0	3.4	13	12.7	28.3	0.9	1.9	1.6	4.4
31	***Prkg1***	G2	---	---	---	11073964	5	0	0.0	7.6	15.3	7.2	28.6	0.9	1.7	1	3.6
32	***Prkg2***	G2	--	--	--	--	1	0	0.0	8.1	15	7	28.5	0.9	1.5	0.8	3.1
33	***Clk4***	S	--	---	---	---	2	0	0.0	6.8	21.5	5.2	33.1	0.9	2.3	0.7	3.9
34	***Ephb2***	S	--	--	--	15973414	6	1	0.2	6.1	21.6	1.4	28.9	0.5	1.6	0.2	2.4
35	***Guk1***	S	--	---	---	---	1	0	0.0	9.4	29.7	4.2	43.1	0.8	2	0.4	3.3
36	***Itgae***	S	--	---	---	---	2	0	0.0	7.4	18.3	1.9	28.2	0.7	1.3	0.3	2.3
37	***Mapkap1***	S	--	--	--	17012250	1	0	0.0	7.5	15.9	3.4	27.1	0.5	1.1	0.3	1.9
38	***Neo1***	S	--	--	--	--	3	0	0.0	7.6	17.3	3.3	28.6	0.7	1.4	0.4	2.5
39	***Ppm1g***	S	--	17054950	--	---	1	1	1.0	6.3	14.8	2.1	23.1	0.5	1	0.2	1.7
40	***Ppm1h***	S	--	---	---	18059182	2	0	0.0	8.6	14.5	1.9	25.5	1.2	2.2	0.4	3.8
41	***Taf9***	S	--	12837753	--	12837753	5	2	0.4	8.1	15.5	2	25.6	1.1	1.7	0.3	3.1
42	***Inpp5f***	S and G2	--	---	---	---	1	0	0.0	9.8	17.5	6.8	34.2	1	1.3	0.5	2.8
43	***Plk1***	S and G2	--	---	15838519:16557283	---	3	3	1.0	9.4	19.3	8.6	36.6	1.1	2	0.7	3.8
										8.4	**13.5**	**4.1**	**26**	**1.5**	**1**	**0.5**	**2.5**

--- ***Role in Cell cycle/Proliferation not well known***

The table provides the classified list of molecules based on their exclusivity for regulation of a particular phase of the cell cycle. Also listed are the ratio of observed versus predicted functions of the hits using GO terms.

Table S4

List of molecules classified as cell cycle targets.

	G1 TARGETS	PMIDs
1	ATM	11544175:8843193
2	ATR	11544175:18606783
3	CCNC	1833066:7568034:9552396:8730095
4	CCND1	19167337
5	CCND2	19167337
6	CCND3	19167337
7	CCNE1	19167337:7797073:8156587
8	CCNE2	19167337:7797073:8156587
9	CCNG1	12556559
10	CCNG2	11956189:9139721
11	CCNH	7533895:9130709
12	CDC25A	14681206:10454565
13	CDC2A	17700700
14	CDC34	8248134:11514588
15	CDC37	8703009:9228064:14701845
16	CDC7	10846177
17	CDK2	19167337
18	CDK4	19167337
19	CDK5	8302605:1358458
20	CDK6	19167337
21	CDK7	9832506:7929589
22	CDK8	9584184:17612495
23	CDKN1C	7729684
24	CDKN2B	19167337
25	CDKN2C	19167337
26	CDKN2D	19167337
27	CHEK1	11544175
28	CHEK2	11544175
29	E2F1	10619603:19603422
30	E2F2	19457859
31	E2F3	15467444
32	E2F4	19585502:19562678
33	E2F5	15467444
34	E2F6	17457055:19549334
35	FOS	17216194
36	HIPK2	12851404
37	JUN	17216194
38	JUNB	18793152
39	MDM2	15485814:8628312:10995885:9087426
40	MNAT1	10026172:11113200
41	MYC	12631706
42	p27	8730099:10385618:8033213
43	PLK2	12651910:12972611
44	RB1	11018009:7777526:9694794
45	RBL1	1152119
46	RBL2	1152119:9188854:8253384
47	TFDP1	14618416:18687693
48	TFDP2	9704927
49	Trp53	7742528:9843965:11884608:10072388
50	Trp63	17114587:14737098
51	TRP73	10562283

	S TARGETS	PMIDs
1	ATM	11544175:8843193
2	ATR	11544175:18606783
3	CCNA1	11566717:19167337
4	CCNA2	11566717:19167337
5	CCNC	1833066:7568034:9552396:8730095
6	CCNE1	19167337:7797073:8156587
7	CCNE2	19167337:7797073:8156587
8	CCNH	7533895:9130709
9	CDC25A	10454565:10995786
10	CDC2A	17635936
11	CDC45L	19054765
12	CDC6	16439999:18687693
13	CDC7	10846177
14	CDK2	19167337
15	CDK7	9832506:7929589
16	CDK8	9584184:17612495
17	CHEK1	11544175
18	CHEK2	11544175
19	E2F1	10619603:19603422
20	E2F2	19457859
21	E2F3	15467444
22	E2F4	19585502:19562678
23	E2F5	15467444
24	E2F6	17457055:19549334
25	FOS	17216194
26	GMNN	19487297:11125146
27	JUN	17216194
28	JUNB	18793152
29	MCM2	17680271
30	MCM3	19064704:19377303
31	MCM4	16754955
32	MCM5	16754955
33	MCM6	16754955
34	MCM7	16754955: 19647517
35	MDM2	15485814:8628312:10995885:9087426
36	MNAT1	10026172:11113200
37	MYC	19554081
38	ORC1L	19197067
39	ORC2L	17680271
40	ORC3L	17716973
41	ORC4L	18652488:19647517
42	ORC5L	17716973
43	ORC6L	17716973
44	PCNA	19595719
45	RB1	11018009:7777526:9694794
46	RBL1	1152119
47	RBL2	1152119:9188854:8253384
48	RIS2	18006686:11125146
49	SKP1A	18353424
50	SKP2	19477924
51	TFDP1	14618416:18687693
52	TFDP2	9704927
53	Trp53	7742528:9843965:11884608:10072388

	G2 TARGETS	PMIDs
1	ANAPC2	11285280
2	ATM	11544175
3	ATR	11544175
4	AURKB	19342897
5	CCNB1	11285280
6	CCNB2	9926943
7	CCNB3	7474080
8	CCNG1	16322753 :18408012
9	CCNH	7533895:9130709
10	CDC16	12629511
11	CDC20	11285280
12	CDC25A	19192479
13	CDC25C	18604163
14	CDC2A	19570916:19013283
15	CDK10	8208557
16	CENPA	18007590
17	CENPB	16183641
18	CENPC	12490152
19	CENPE	9763420
20	CENPH	16875666
21	CHEK1	11544175
22	CHEK2	11544175
23	MAD2L1	19461085
24	MAD2L2	10366450
25	p27	17954563: 16310807
26	PLK1	19033445
27	PLK2	19001868
28	PLK3	11971976
29	STK6	19342897

List of molecules classified as cell cycle targets.

Table S4 provides the complete details of classification of molecules according to their functional role in cell cycle and their corresponding PMID for the literature evidence.

Table S6

Occurrences of nodes in shortest path networks.

G1 Phase			S Phase			G2 Phase			G1S Phase		
Molecule	No. of occurances	Score	Molecule	No. of occurances	Score	Molecule	No. of occurances	Score	Molecule	No. of occurances	Score
TRP53	612	10.8	TRP53	372	8.2	LASP1	175	8.9	CDK2	833	11.4
RB1	471	8.3	ITGB7	367	8.1	PRKD1	159	8.1	TRP53	648	8.8
PTK2B	457	8.0	NTN1	278	6.1	TRP53	137	7.0	ABL1	465	6.3
PRKCA	385	6.8	ADORA2B	278	6.1	PRKCA	126	6.4	POLD1	463	6.3
TRAF6	332	5.8	FOS	229	5.0	CDK7	74	3.7	ANXA1	434	5.9
TICAM2	332	5.8	ABL1	225	4.9	FZR1	60	3.0	CREB1	424	5.8
KIF23	316	5.5	YWHAG	204	4.5	EGFR	59	2.9	PRKG1	391	5.3
YWHAQ	313	5.5	PIN1	201	4.4	POLD1	55	2.7	GRB2	388	5.3
BCL2	266	4.6	TRAF6	190	4.1	CDK2	46	2.3	EGFR	344	4.7
CDK2	258	4.5	CSE1L	189	4.1	CHEK2	41	2.0	CREBBP	311	4.2
IKBKAP	251	4.4	CDK2	177	3.9	ETS2	40	2.0	RIS2	294	4.0
MAPK8	234	4.1	DOK1	154	3.3	PRKG1	34	1.7	PRKCA	289	3.9
ESR1	195	3.4	DCC	151	3.3	AREG	34	1.7	SRC	273	3.7
POLD1	192	3.3	AREG	141	3.0	CASP3	31	1.5	RB1	268	3.6
PTEN	191	3.3	POLD1	138	3.0	NFE2L2	28	1.3	UBB	260	3.5
CREBBP	184	3.2	RIS2	138	3.0	CREBBP	27	1.3	AKT1	238	3.2
AKT1	178	3.1	STAT1	138	3.0	ACTB	26	1.2	EP300	236	3.2
EP300	169	2.9	E7	135	2.9	HDAC1	25	1.2	BRCA1	230	3.1
MCM7	160	2.8	EZR	128	2.8	CTNNB1	25	1.2	MCM7	230	3.1
SRC	153	2.6	PKM2	127	2.7	CREB1	24	1.1	ESR1	212	2.8
AREG	147	2.5	MCM7	125	2.7	UBTF	23	1.1	CTNNB1	191	2.6
EPC1	146	2.5	BRCA1	106	2.3	SYK	22	1.0	POLR2A	181	2.4
UBB	145	2.5	PRKCA	103	2.2	ZYX	21	1.0	STAT1	180	2.4
POLR2A	130	2.2	SMAD3	99	2.1	ESR1	21	1.0	MAPK3	174	2.3
ARHGEF7	124	2.1	RB1	93	2.0	NR3C1	20	0.9	CCNA2	166	2.2
ZBTB17	118	2.0	EED	82	1.7	MNAT1	19	0.9	AREG	165	2.2
BRCA1	115	2.0	TAF1	75	1.6	YWHAQ	19	0.9	LYN	162	2.2
EEF1D	115	2.0	POLR2A	75	1.6	IKBKAP	19	0.9	GADD45G	152	2.0
CASP3	114	2.0	EP300	70	1.5	GTF2I	18	0.8	SKP2	149	2.0
GRB2	103	1.8	UBB	70	1.5	DIAPH2	18	0.8	CDKN1B	148	2.0
SYNGAP1	100	1.7	RBL1	70	1.5	APC	18	0.8	CSNK2A1	137	1.8
RAF1	95	1.6	CCNA2	68	1.4	SYNGAP1	17	0.8	ELK1	136	1.8
WT1	94	1.6	RAF1	67	1.4	CDC20	17	0.8	JUN	136	1.8
CSNK2A1	94	1.6	DAB1	67	1.4	DLGAP4	17	0.8	CDC25A	136	1.8
TICAM1	92	1.6	ETF1	67	1.4	PPP1R14A	16	0.7	TOPBP1	127	1.7
NFKBIA	92	1.6	GRIN2B	66	1.4	MAPK8	16	0.7	E2F1	126	1.7
ABL1	90	1.5	COIL	66	1.4	ACTC1	15	0.7	TUBA4A	119	1.6
E2F1	89	1.5	MAPK1	65	1.4	E6	15	0.7	MYC	119	1.6
DLGAP4	89	1.5	CREBBP	60	1.2	RHOD	14	0.6	EPC1	114	1.5
MYC	89	1.5	ABL2	56	1.2	AKT1	14	0.6	CASP3	113	1.5
LCK	88	1.5	CASP3	56	1.2	MAPK1	14	0.6	WT1	105	1.4
XRCC6	86	1.5	MCM3	55	1.1	UBB	12	0.5	PTPN2	104	1.4
TANK	86	1.5	EPC1	55	1.1	BRCA1	12	0.5	CCND1	103	1.3
TRIM27	82	1.4	JUN	54	1.1	ITPR1	12	0.5	ARHGEF7	100	1.3
MAPK1	80	1.3	CDK5	51	1.0	ATR	12	0.5	YWHAE	100	1.3
PRC1	76	1.3	YWHAE	51	1.0	CSNK2A1	12	0.5	GADD45A	98	1.3
RACGAP1	76	1.3	EGFR	50	1.0	RB1	12	0.5	PCNA	96	1.3
SMAD3	76	1.3	E2F1	49	1.0	TUBA4A	11	0.5	MCM5	94	1.2
YWHAE	71	1.2	MCM5	46	0.9	CIB1	11	0.5	ZBTB17	93	1.2
LIMA1	71	1.2	ESR1	44	0.9	SHC	11	0.5	PPP2R4	90	1.2
CDKN1B	70	1.2	LYN	42	0.8	MCM7	11	0.5	PITPNM1	88	1.1
MRGBP	64	1.1	MYC	42	0.8	NPM1	11	0.5	MAPT	77	1.0
CCNA2	63	1.0	TOPBP1	40	0.8	PPP1CA	11	0.5	PRKCD	76	1.0
PCNA	62	1.0	RBL2	40	0.8	STAT3	10	0.4	MAPK8	75	1.0
MNAT1	61	1.0	UBA1	39	0.8	ABL1	10	0.4	GTF2I	74	0.9
MDM4	59	1.0	ITGA4	36	0.7	IQGAP1	9	0.4	ORC1L	72	0.9
MYOD1	58	1.0	AKT1	35	0.7	ACTA1	8	0.3	MAPK14	70	0.9
CDK5	57	0.9	PICK1	35	0.7	WAS	8	0.3	CDK5	70	0.9
ATM	57	0.9	SRC	34	0.7	XRCC6	8	0.3	TRIM27	68	0.9
RBL1	57	0.9	TRIM27	33	0.6	CCNA2	8	0.3	RBL1	67	0.9
MDM2	56	0.9	SKP2	33	0.6	CSNK1A1	8	0.3	CHKA	65	0.8

EGFR	56	0.9	**VHL**	33	0.6	**HDAC2**	8	0.3	**E7**	64	0.8
RBL2	55	0.9	**LCK**	32	0.6	**SKP1A**	7	0.3	**KRT8**	63	0.8
CREM	55	0.9	**ORC1L**	32	0.6	**MDC1**	7	0.3	**MYOD1**	62	0.8
GSK3B	52	0.9	**PPP2CA**	32	0.6	**CDC25B**	7	0.3	**NPM1**	60	0.8
PPP2R4	51	0.8	**TLN1**	28	0.5	**MYC**	7	0.3	**NFKBIA**	59	0.7
SMAD2	51	0.8	**CTNNB1**	28	0.5	**MAPK3**	7	0.3	**SMAD3**	56	0.7
CTNNB1	51	0.8	**TFDP2**	27	0.5	**MDM4**	7	0.3	**STAT3**	55	0.7
PAK4	49	0.8	**PTK2**	27	0.5	**BUB1B**	7	0.3	**XPO1**	54	0.7
FGFR1	48	0.8	**TFDP1**	26	0.5	**TOP1**	7	0.3	**IKBKAP**	54	0.7
SHC	47	0.8	**XPO1**	26	0.5	**NCK1**	6	0.2	**MAP3K3**	52	0.6
CHKA	47	0.8	**NME6**	25	0.5	**PMVK**	6	0.2	**DLGAP4**	52	0.6
ATR	44	0.7	**ORC2L**	25	0.5	**PLCG2**	6	0.2	**PPP1CA**	52	0.6
KAT5	43	0.7	**CDKN1B**	24	0.4	**PCNA**	6	0.2	**SYNGAP1**	51	0.6
STAT3	42	0.7	**PPP1CA**	24	0.4	**PIK3R1**	6	0.2	**MCM3**	49	0.6
PIAS4	41	0.7	**YY1**	23	0.4	**HAND2**	6	0.2	**MAPK1**	47	0.6
CCND1	40	0.6	**MNAT1**	23	0.4	**PLCG1**	6	0.2	**HIST3H3**	47	0.6
BIRC6	39	0.6	**CDK9**	23	0.4	**ATM**	6	0.2	**MRGBP**	46	0.6
JUN	39	0.6	**MAPT**	23	0.4	**JUN**	6	0.2	**NR3C1**	46	0.6
PLK1	38	0.6	**HDAC1**	22	0.4	**DAXX**	6	0.2	**FHL2**	46	0.6
MAPK14	38	0.6	**MRGBP**	22	0.4	**SRC**	6	0.2	**YWHAB**	46	0.6
E7	38	0.6	**ACP1**	21	0.4	**HSP90AA1**	6	0.2	**MNAT1**	44	0.5
LYN	37	0.6	**ARHGEF7**	21	0.4	**PARP1**	6	0.2	**CDK4**	43	0.5
BCL2L1	37	0.6	**DNMT1**	21	0.4	**PRKAR2B**	5	0.2	**GSK3B**	43	0.5
FHL2	37	0.6	**XRCC6**	21	0.4	**STK11**	5	0.2	**CSNK1D**	42	0.5
NR3C1	36	0.6	**MAPK3**	21	0.4	**NEDD9**	5	0.2	**SHC**	41	0.5
CHEK2	35	0.6	**MCC**	21	0.4	**SMARCA4**	5	0.2	**PLK1**	41	0.5
MAPK9	34	0.5	**NCOA3**	20	0.4	**EIF4EBP1**	5	0.2	**CCNE1**	41	0.5
SLC6A4	33	0.5	**CDC2L1**	20	0.4	**THRA**	5	0.2	**SMARCA4**	41	0.5
TFDP2	32	0.5	**DNMT3A**	20	0.4	**LCK**	4	0.1	**MCM4**	38	0.5
CDK4	32	0.5	**PKN2**	20	0.4	**BLM**	4	0.1	**CSNK1A1**	38	0.5
SNCA	32	0.5	**CSNK2B**	19	0.3	**CDK5**	4	0.1	**SMAD2**	37	0.4
TFDP1	30	0.5	**SP1**	19	0.3	**TGM2**	4	0.1	**SP1**	37	0.4
CASP8	30	0.5	**TBP**	19	0.3	**AKAP1**	4	0.1	**PIK3R1**	37	0.4
EPHA4	30	0.5	**CCNA1**	18	0.3	**PLK1**	4	0.1	**LCK**	36	0.4
UBE2I	29	0.4	**CSNK1A1**	18	0.3	**FHOD1**	4	0.1	**DGKZ**	36	0.4
UBC	29	0.4	**RELA**	18	0.3	**ITGB3**	4	0.1	**TFDP1**	35	0.4
GADD45G	28	0.4	**LRRC59**	18	0.3	**CCND1**	4	0.1	**ORC2L**	35	0.4
HDAC1	28	0.4	**DDB1**	17	0.3	**GRB2**	4	0.1	**KIT**	35	0.4
HSP90AA1	28	0.4	**GNB2L1**	17	0.3	**BCL2**	4	0.1	**MAP2K1**	35	0.4
DYNLL1	27	0.4	**HDAC2**	17	0.3	**NDC80**	4	0.1	**KPNA2**	34	0.4
DGKZ	27	0.4	**EPB41**	16	0.3	**CDC25C**	4	0.1	**XRCC6**	34	0.4
MED29	25	0.4	**SMAD2**	16	0.3	**CHKA**	4	0.1	**ITPR1**	34	0.4
PRG2	25	0.4	**RAD52**	16	0.3	**HSP90AB1**	4	0.1	**HSP90AA1**	34	0.4
LRRC59	25	0.4	**SUV39H1**	16	0.3	**BUB1**	4	0.1	**PKN2**	33	0.4
MAPT	25	0.4	**MCM4**	16	0.3	**PPP1R9B**	4	0.1	**TFDP2**	32	0.4
YWHAZ	25	0.4	**NEK6**	16	0.3	**VAV1**	4	0.1	**BCL2**	32	0.4
BLM	25	0.4	**GADD45G**	15	0.2	**NCKIPSD**	4	0.1	**S100B**	32	0.4
AATF	25	0.4	**TAF11**	15	0.2	**ACTN4**	3	0.1	**CREM**	32	0.4
CCNA1	24	0.4	**MED9**	15	0.2	**PITPNA**	3	0.1	**EPB41**	31	0.4
TOP2A	24	0.4	**TCF7L2**	14	0.2	**EP300**	3	0.1	**UBE2I**	31	0.4
HDAC2	24	0.4	**GLCE**	14	0.2	**INSR**	3	0.1	**TUBB**	31	0.4
TFAP2A	24	0.4	**DUT**	14	0.2	**VASP**	3	0.1	**RPS6KB1**	31	0.4
CRK	24	0.4	**UBC**	14	0.2	**RAF1**	3	0.1	**MAP3K7**	30	0.3
PDPK1	24	0.4	**MED1**	13	0.2	**PTPN1**	3	0.1	**TRP73**	30	0.3
GART	24	0.4	**SORBS2**	13	0.2	**MAP3K7**	3	0.1	**NCOA6**	30	0.3
PPP1CA	24	0.4	**CDC25A**	13	0.2	**MAP3K3**	3	0.1	**MED29**	28	0.3
MAP3K3	23	0.3	**ITGB5**	12	0.2	**TELO2**	3	0.1	**NCK1**	28	0.3
FGF8	23	0.3	**CENPJ**	11	0.2	**PALM**	3	0.1	**RBL2**	28	0.3
RELA	23	0.3	**KIT**	11	0.2	**BRCA2**	3	0.1	**MAPK8IP3**	27	0.3
HSPA8	23	0.3	**NCOA2**	11	0.2	**MIS12**	3	0.1	**PRKAR1A**	26	0.3
PTPN2	23	0.3	**MPP1**	11	0.2	**KPNA3**	3	0.1	**ATM**	26	0.3
TBP	23	0.3	**GADD45A**	11	0.2	**HIST3H3**	3	0.1	**RPS6KA3**	26	0.3
FLNA	23	0.3	**CDC5L**	11	0.2	**CDKN1B**	3	0.1	**IGF1R**	25	0.3
PML	22	0.3	**PRKCB1**	11	0.2	**PTP4A3**	3	0.1	**ATR**	25	0.3
MED1	22	0.3	**PITPNM1**	11	0.2	**FRAP1**	3	0.1	**CDC6**	25	0.3
CDC2L5	22	0.3	**YWHAB**	11	0.2	**CCNB1IP1**	3	0.1	**CRK**	25	0.3
CDC2L1	21	0.3	**LMNA**	10	0.1	**KAT5**	3	0.1	**PTP4A3**	25	0.3
SORBS2	21	0.3	**PARD3**	10	0.1	**E2F1**	3	0.1	**SMAD4**	25	0.3
CTBP1	21	0.3	**CAPN1**	10	0.1	**CALM1**	3	0.1	**E6**	25	0.3
YAP1	21	0.3	**PTPN2**	10	0.1	**CRIP2**	3	0.1	**MDM4**	25	0.3

TRAF1	20	0.3	**HCFC1**	10	0.1	**CRKL**	3	0.1	**PIN1**	24	0.3
MAP3K7	20	0.3	**CCNH**	10	0.1	**FLNA**	3	0.1	**RAF1**	24	0.3
PITPNM1	20	0.3	**SIAH1**	10	0.1	**PTPN13**	3	0.1	**DDB1**	23	0.2
CDC25B	19	0.3	**MAPK14**	9	0.1	**HIST1H3C**	3	0.1	**SLC6A4**	23	0.2
CCNH	19	0.3	**PFAS**	9	0.1	**MARK3**	3	0.1	**RAD52**	23	0.2
MED6	19	0.3	**NCOR2**	9	0.1	**MAD2L2**	3	0.1	**CDC7**	23	0.2
PCAF	18	0.2	**ITGB3**	9	0.1	**POLR2A**	3	0.1	**MYBL2**	22	0.2
GADD45A	18	0.2	**TRP73**	9	0.1	**PITPNM1**	3	0.1	**CCNH**	22	0.2
SP1	18	0.2	**ATM**	9	0.1	**YWHAB**	3	0.1	**SNCA**	22	0.2
NPM1	18	0.2	**BCL2**	9	0.1	**HDAC3**	3	0.1	**KAT5**	22	0.2
STK11	18	0.2	**CRKL**	9	0.1	**YY1**	2	0.0	**TBP**	22	0.2
NCK1	18	0.2	**E6**	9	0.1	**IL16**	2	0.0	**VAV1**	22	0.2
BMPR1B	18	0.2	**PRKCD**	9	0.1	**VCL**	2	0.0	**TOP2A**	21	0.2
E6	18	0.2	**MDM4**	9	0.1	**NCOA3**	2	0.0	**CDX2**	21	0.2
MDC1	17	0.2	**MYOD1**	9	0.1	**KDR**	2	0.0	**MAPK9**	21	0.2
EPB41	17	0.2	**ROCK1**	8	0.1	**RAC1**	2	0.0	**IRS1**	20	0.2
RIPK1	17	0.2	**SLC33A1**	8	0.1	**MAFG**	2	0.0	**MCM6**	20	0.2
CDC25C	17	0.2	**CRK**	8	0.1	**RAD1**	2	0.0	**TP73L**	19	0.2
FOXO1	17	0.2	**MED29**	8	0.1	**PPP2R4**	2	0.0	**MED1**	19	0.2
PFAS	16	0.2	**ITGB2**	8	0.1	**CDC2L5**	2	0.0	**HDAC1**	19	0.2
PTPN12	16	0.2	**KAT5**	8	0.1	**CCNB1**	2	0.0	**GADD45B**	19	0.2
CHEK1	16	0.2	**CDKN2A**	8	0.1	**RAD51**	2	0.0	**GNB2L1**	18	0.2
VIM	16	0.2	**NF2**	8	0.1	**VIM**	2	0.0	**CSK**	18	0.2
MAP2K1	16	0.2	**NFATC2**	8	0.1	**PRKAR1A**	2	0.0	**CDC2L5**	18	0.2
ELF3	15	0.2	**NUMB**	8	0.1	**LYN**	2	0.0	**PTPN1**	17	0.2
SLC9A3	15	0.2	**VDR**	7	0.1	**GDNF**	2	0.0	**PML**	17	0.2
GTF2I	15	0.2	**PML**	7	0.1	**PSMA3**	2	0.0	**RPS6KA1**	17	0.2
RUVBL1	15	0.2	**USF2**	7	0.1	**SUMO2**	2	0.0	**MED6**	17	0.2
VHL	15	0.2	**DAB2**	7	0.1	**GADD45A**	2	0.0	**LASP1**	17	0.2
FGFR3	14	0.2	**SDCBP**	7	0.1	**BAD**	2	0.0	**PLCG2**	16	0.2
PSMD10	14	0.2	**RUVBL1**	7	0.1	**ASF1A**	2	0.0	**RXRA**	16	0.2
PKN1	14	0.2	**MED6**	7	0.1	**PCYT1A**	2	0.0	**CDC25C**	16	0.2
RAD17	14	0.2	**GSK3B**	7	0.1	**TRP73**	2	0.0	**PKN1**	16	0.2
CLSPN	14	0.2	**CAMK2G**	7	0.1	**YWHAE**	2	0.0	**POLA1**	16	0.2
CSNK1D	14	0.2	**KCNK3**	6	0.0	**ARRB1**	2	0.0	**YY1**	16	0.2
TNFAIP3	14	0.2	**DGKZ**	6	0.0	**FOS**	2	0.0	**JAK1**	16	0.2
CDC25A	14	0.2	**RPS6KA1**	6	0.0	**DCLK1**	2	0.0	**UBTF**	16	0.2
NBN	13	0.2	**PALM**	6	0.0	**TOP2A**	2	0.0	**HRAS**	16	0.2
TP73L	13	0.2	**HLA-B**	6	0.0	**BCL2L1**	2	0.0	**KHDRBS1**	16	0.2
SMN1	13	0.2	**RXRA**	6	0.0	**HNRNPU**	2	0.0	**CDC2L1**	15	0.1
YWHAH	13	0.2	**STAT3**	6	0.0	**ESR2**	2	0.0	**PSMD10**	15	0.1
CDC42	13	0.2	**PTPN11**	6	0.0	**RELA**	2	0.0	**MED9**	15	0.1
TRP73	13	0.2	**HIST3H3**	6	0.0	**SMC1A**	2	0.0	**NEK6**	15	0.1
TGFB1I1	13	0.2	**EZH2**	6	0.0	**HSPA8**	2	0.0	**SET**	15	0.1
SH2D3C	13	0.2	**DNMT3B**	6	0.0	**STMN1**	2	0.0	**VPS72**	15	0.1
FRAP1	13	0.2	**TOP2A**	6	0.0	**EGR1**	2	0.0	**CSNK2B**	15	0.1
SMAD4	13	0.2	**POLR2E**	6	0.0	**CREM**	2	0.0	**CDC5L**	15	0.1
CASP2	13	0.2	**CAMK2D**	6	0.0	**REPS1**	2	0.0	**TRAF6**	14	0.1
RAD9	13	0.2	**WWOX**	6	0.0	**PPP1R12A**	2	0.0	**ITGB4**	14	0.1
MST1R	12	0.1	**CDC25C**	6	0.0	**MYOD1**	2	0.0	**EZR**	14	0.1
PALM	12	0.1	**MED10**	6	0.0	**VDR**	1	-0.1	**DAPP1**	14	0.1
BIRC5	12	0.1	**CHKA**	6	0.0	**POLA1**	1	-0.1	**MED28**	14	0.1
IKBKB	12	0.1	**CSNK2A1**	6	0.0	**ANXA2**	1	-0.1	**RAD17**	14	0.1
HDAC5	12	0.1	**GTF2B**	6	0.0	**AURKB**	1	-0.1	**SGK1**	14	0.1
PIN1	12	0.1	**E2**	6	0.0	**PPP1R1B**	1	-0.1	**FZR1**	14	0.1
IRF3	12	0.1	**CDC7**	6	0.0	**MCM3**	1	-0.1	**PALM**	13	0.1
RIS2	12	0.1	**MED28**	6	0.0	**SPIB**	1	-0.1	**PCAF**	13	0.1
RUNX1	12	0.1	**ZBTB17**	6	0.0	**SLC4A1**	1	-0.1	**PPM1B**	13	0.1
ITGB3	12	0.1	**TARS**	5	0.0	**RNPS1**	1	-0.1	**PLCG1**	13	0.1
RUVBL2	12	0.1	**NGFR**	5	0.0	**ARRB2**	1	-0.1	**ARID3A**	13	0.1
PARP1	12	0.1	**ITGB1**	5	0.0	**BID**	1	-0.1	**MED10**	13	0.1
EPPK1	11	0.1	**JAK2**	5	0.0	**ILK**	1	-0.1	**PPP2CA**	13	0.1
CCNG1	11	0.1	**TERF2**	5	0.0	**KLF1**	1	-0.1	**PDGFRB**	13	0.1
ARID3A	11	0.1	**PLK1**	5	0.0	**EIF2AK2**	1	-0.1	**TOP2B**	13	0.1
SMC1A	11	0.1	**KCNK9**	5	0.0	**TPT1**	1	-0.1	**APEX1**	13	0.1
MRE11A	11	0.1	**BAD**	5	0.0	**GTF2A1**	1	-0.1	**MDM2**	12	0.1
NGFR	11	0.1	**GTF2F1**	5	0.0	**PNKP**	1	-0.1	**TAF1**	12	0.1
IRF7	11	0.1	**BCR**	5	0.0	**JUP**	1	-0.1	**E2**	12	0.1
PRKAR1A	11	0.1	**CABLES1**	5	0.0	**DCLK3**	1	-0.1	**TERT**	12	0.1
CSNK1A1	11	0.1	**CDK8**	5	0.0	**PTPN18**	1	-0.1	**KRT18**	12	0.1

ARRB2	10	0.1	**SMARCB1**	5	0.0	**EXOC4**	1	-0.1	**ACTB**	12	0.1
RGS3	10	0.1	**STAT5B**	5	0.0	**RGS20**	1	-0.1	**STK11**	12	0.1
PAK6	10	0.1	**POU2F1**	5	0.0	**PRKCZ**	1	-0.1	**CDKN2A**	12	0.1
EIF4EBP1	10	0.1	**CCNT1**	5	0.0	**LMNB1**	1	-0.1	**PIAS1**	12	0.1
CHD4	10	0.1	**GART**	5	0.0	**UNC13D**	1	-0.1	**AXIN1**	11	0.1
HSF1	10	0.1	**ERCC3**	5	0.0	**RPS6KA1**	1	-0.1	**CHEK1**	11	0.1
MED9	10	0.1	**RUVBL2**	5	0.0	**EPS8**	1	-0.1	**DCLK1**	11	0.1
THRA	10	0.1	**KCNK15**	5	0.0	**LZTS1**	1	-0.1	**MAPK10**	11	0.1
POLA1	10	0.1	**CHD4**	5	0.0	**COPS5**	1	-0.1	**THRA**	11	0.1
PAICS	10	0.1	**EXOS**	5	0.0	**RBBP4**	1	-0.1	**SIAH1**	11	0.1
ITGB4	9	0.1	**ANXA2**	4	0.0	**CENPB**	1	-0.1	**VDR**	10	0.1
SMARCB1	9	0.1	**SUMO1**	4	0.0	**REV3L**	1	-0.1	**ROCK1**	10	0.1
RHEB	9	0.1	**IER3**	4	0.0	**KRT8**	1	-0.1	**CCNA1**	10	0.1
IRS1	9	0.1	**TUBA4A**	4	0.0	**CTNNA1**	1	-0.1	**KDR**	10	0.1
MED10	9	0.1	**PDGFRB**	4	0.0	**SLK**	1	-0.1	**SYN1**	10	0.1
ADCY6	9	0.1	**EPPK1**	4	0.0	**PFKFB2**	1	-0.1	**CDK7**	10	0.1
PSMC6	9	0.1	**MITF**	4	0.0	**JAK2**	1	-0.1	**CHEK2**	10	0.1
TARS	9	0.1	**STK11**	4	0.0	**ARHGEF7**	1	-0.1	**CHD4**	10	0.1
FGF13	9	0.1	**INSR**	4	0.0	**PDPK1**	1	-0.1	**TIAM1**	10	0.1
CASP9	9	0.1	**AKAP13**	4	0.0	**SNRP70**	1	-0.1	**BLM**	10	0.1
ATXN1	9	0.1	**BLM**	4	0.0	**DMD**	1	-0.1	**CCND2**	10	0.1
NCOA2	9	0.1	**PAICS**	4	0.0	**VPS72**	1	-0.1	**CABLES1**	10	0.1
TJP2	9	0.1	**PRAM1**	4	0.0	**RGS3**	1	-0.1	**E2F5**	10	0.1
FZR1	9	0.1	**PCAF**	4	0.0	**GRK5**	1	-0.1	**SMARCE1**	10	0.1
PNKP	8	0.1	**TAF7**	4	0.0	**AKAP8**	1	-0.1	**RFC2**	9	0.1
TELO2	8	0.1	**SLK**	4	0.0	**BIRC6**	1	-0.1	**MAP3K5**	9	0.1
PA2G4	8	0.1	**PFKFB2**	4	0.0	**POU5F1**	1	-0.1	**PTK2**	9	0.1
LLGL1	8	0.1	**PIK3R1**	4	0.0	**CGN**	1	-0.1	**ID2**	9	0.1
CTBP2	8	0.1	**ASCC3L1**	4	0.0	**HSPA9**	1	-0.1	**CD5**	9	0.1
PHB2	8	0.1	**WDR8**	4	0.0	**ARHGAP1**	1	-0.1	**CASP9**	9	0.1
RAD51	8	0.1	**AKAP8**	4	0.0	**BCR**	1	-0.1	**CTBP1**	9	0.1
HLA-B	8	0.1	**MAP3K2**	4	0.0	**FUSIP1**	1	-0.1	**CASP4**	9	0.1
PIK3R1	8	0.1	**ERBB2**	4	0.0	**TBPL1**	1	-0.1	**PAX2**	9	0.1
VPS72	8	0.1	**TOP2B**	4	0.0	**MVD**	1	-0.1	**RUVBL2**	9	0.1
BAD	8	0.1	**CHEK1**	4	0.0	**ERBB2**	1	-0.1	**SPNS1**	9	0.1
PRKDC	8	0.1	**PTP4A3**	4	0.0	**LIG4**	1	-0.1	**SRF**	9	0.1
LMNA	8	0.1	**AATF**	4	0.0	**GSK3A**	1	-0.1	**CDK9**	8	0.0
CDKN2A	8	0.1	**CDC20**	4	0.0	**NFKBIA**	1	-0.1	**SMARCB1**	8	0.0
PAX2	8	0.1	**E2F5**	4	0.0	**CBX5**	1	-0.1	**CCNG1**	8	0.0
RBP1	8	0.1	**PPP2R1A**	4	0.0	**PTK2**	1	-0.1	**PAG1**	8	0.0
CCNT2	8	0.1	**CASP4**	4	0.0	**E7**	1	-0.1	**TUBA3C**	8	0.0
NCOA6	8	0.1	**ATR**	4	0.0	**PAK6**	1	-0.1	**HSF1**	8	0.0
VDR	7	0.1	**BCL2L1**	4	0.0	**CHEK1**	1	-0.1	**TUBA1B**	8	0.0
IRAK1	7	0.1	**DAXX**	4	0.0	**SFN**	1	-0.1	**BAD**	8	0.0
EIF2AK2	7	0.1	**HSP90AB1**	4	0.0	**PRG2**	1	-0.1	**FHL5**	8	0.0
U2AF2	7	0.1	**CHEK2**	4	0.0	**SNCA**	1	-0.1	**DBNL**	7	0.0
SQSTM1	7	0.1	**PIAS1**	4	0.0	**CSNK1D**	1	-0.1	**IER2**	7	0.0
EIF3A	7	0.1	**NCOA6**	4	0.0	**KHDRBS1**	1	-0.1	**MCRS1**	7	0.0
PRKCI	7	0.1	**RET**	4	0.0	**RHEB**	1	-0.1	**PPP3R1**	7	0.0
DCLK1	7	0.1	**AHR**	4	0.0	**GAPDH**	1	-0.1	**FOXM1**	7	0.0
COIL	7	0.1	**E2F2**	4	0.0	**XRCC1**	1	-0.1	**FAS**	7	0.0
NUMB	7	0.1	**FZR1**	4	0.0	**PRKA4**	1	-0.1	**SYK**	7	0.0
LIN9	7	0.1	**HCK**	3	0.0	**GPI**	1	-0.1	**CCNT1**	7	0.0
EWSR1	7	0.1	**ZAP70**	3	0.0	**ASF1B**	1	-0.1	**THRB**	7	0.0
ITPR1	7	0.1	**DUSP12**	3	0.0	**GNA12**	1	-0.1	**RPS27A**	7	0.0
DNMT3A	7	0.1	**PTEN**	3	0.0	**ERCC3**	1	-0.1	**ORC3L**	7	0.0
UBTF	7	0.1	**EWSR1**	3	0.0	**SPTBN1**	1	-0.1	**JAG1**	7	0.0
HRAS	7	0.1	**GRB10**	3	0.0	**PSEN2**	1	-0.1	**IKBKE**	7	0.0
PHB	7	0.1	**PRKCG**	3	0.0	**STMN2**	1	-0.1	**LRRC59**	7	0.0
KHDRBS1	7	0.1	**ZMYND11**	3	0.0	**SLC9A3R2**	1	-0.1	**STAT5A**	7	0.0
SMARCE1	7	0.1	**GTF2I**	3	0.0	**STK4**	1	-0.1	**PIM1**	7	0.0
CCND3	7	0.1	**NCK1**	3	0.0	**RIS2**	1	-0.1	**MPP3**	7	0.0
RARA	6	0.0	**NEDD9**	3	0.0	**PRDX1**	1	-0.1	**RAD1**	7	0.0
TBK1	6	0.0	**JAK1**	3	0.0	**NUF2**	1	-0.1	**JAK2**	7	0.0
NCOR2	6	0.0	**PKD1**	3	0.0	**AP3B2**	1	-0.1	**LMNA**	7	0.0
RASGRF1	6	0.0	**STK6**	3	0.0	**BRAF**	1	-0.1	**GART**	7	0.0
FADD	6	0.0	**PCNA**	3	0.0	**COPS3**	1	-0.1	**RANBP9**	7	0.0
MAP3K14	6	0.0	**NOLC1**	3	0.0	**VAV3**	1	-0.1	**VHL**	7	0.0
CAPN1	6	0.0	**TJP2**	3	0.0	**GORASP1**	1	-0.1	**MST1R**	6	0.0
MAPK3	6	0.0	**XRCC5**	3	0.0	**MCL1**	1	-0.1	**SUMO1**	6	0.0

DAXX	6	0.0	**PRKAB1**	3	0.0	**CHD4**	1	-0.1	**RARA**	6	0.0
PRKCD	6	0.0	**PLCG1**	3	0.0	**PRKCD**	1	-0.1	**CD79A**	6	0.0
MED28	6	0.0	**UBQLN4**	3	0.0	**SRF**	1	-0.1	**MEF2A**	6	0.0
E4F1	6	0.0	**PRKDC**	3	0.0	**ADCY6**	1	-0.1	**GPI**	6	0.0
ACTB	6	0.0	**POLR2F**	3	0.0	**ID2**	1	-0.1	**FEN1**	6	0.0
YY1	6	0.0	**TGFB1I1**	3	0.0	**PTBP1**	1	-0.1	**CCNE2**	6	0.0
SHANK2	6	0.0	**ARID3A**	3	0.0	**RGS19**	1	-0.1	**RELA**	6	0.0
LYST	6	0.0	**SMAD4**	3	0.0	**CFTR**	1	-0.1	**RAD51**	6	0.0
IKBKG	6	0.0	**NPM1**	3	0.0	**RAD9**	1	-0.1	**NOLC1**	6	0.0
SH3KBP1	6	0.0	**ORC6L**	3	0.0	**PTPN2**	1	-0.1	**CUX1**	6	0.0
RPS6KA1	6	0.0	**SLC9A3R2**	3	0.0	**RPS6KA3**	1	-0.1	**GRIN2A**	6	0.0
SGK1	6	0.0	**ORC3L**	3	0.0	**PKN1**	1	-0.1	**NF2**	6	0.0
JAK2	6	0.0	**VCP**	3	0.0	**TFAP2A**	1	-0.1	**APP**	6	0.0
CHUK	6	0.0	**PSMD10**	3	0.0	**HNRNPC**	1	-0.1	**CSF2RB**	6	0.0
PFTK1	6	0.0	**CDC6**	3	0.0	**CRMP1**	1	-0.1	**PARP1**	6	0.0
ARRB1	6	0.0	**SMC1A**	3	0.0	**CDC37**	1	-0.1	**DUSP19**	5	0.0
STAT1	6	0.0	**VAV1**	3	0.0	**ZFYVE9**	1	-0.1	**FCGR2A**	5	0.0
MAST1	6	0.0	**STAT5A**	3	0.0	**ERCC6**	1	-0.1	**MDC1**	5	0.0
DCLRE1C	6	0.0	**MTA1**	3	0.0	**PDE3B**	1	-0.1	**RB1CC1**	5	0.0
YWHAB	6	0.0	**PSMC6**	3	0.0	**RAD17**	1	-0.1	**SMARCC1**	5	0.0
SUMO1	5	0.0	**ITGB3BP**	3	0.0	**SIAH1**	1	-0.1	**FLCN**	5	0.0
HIST3H3	5	0.0	**RAD17**	3	0.0	**YWHAZ**	1	-0.1	**STX1A**	5	0.0
SMARCA4	5	0.0	**ACTB**	2	0.0	**SYNJ2BP**	1	-0.1	**WDR8**	5	0.0
LRP2	5	0.0	**CD44**	2	0.0	**CDC25A**	1	-0.1	**AKAP1**	5	0.0
CDC2L6	5	0.0	**PLSCR4**	2	0.0	**EDD**	1	-0.1	**MED17**	5	0.0
TERT	5	0.0	**MTHFD1**	2	0.0	**PKN2**	1	-0.1	**PLEC1**	5	0.0
IKBKE	5	0.0	**GTF2F2**	2	0.0				**CASP10**	5	0.0
MED14	5	0.0	**CTNND2**	2	0.0				**STAT5B**	5	0.0
MYBL2	5	0.0	**CDK6**	2	0.0				**CDC2L6**	5	0.0
SLC9A3R1	5	0.0	**MAST2**	2	0.0				**FBL**	5	0.0
WRN	5	0.0	**AXIN1**	2	0.0				**LIN9**	5	0.0
NEK6	5	0.0	**ID3**	2	0.0				**PA2G4**	5	0.0
SP3	5	0.0	**CXORF53**	2	0.0				**NUAK1**	5	0.0
PDGFRB	5	0.0	**CDC2L5**	2	0.0				**DOK4**	5	0.0
TH	5	0.0	**SLC6A4**	2	0.0				**IER3**	5	0.0
ZMYND11	5	0.0	**SHC**	2	0.0				**CDK6**	5	0.0
INSR	5	0.0	**TUBA1A**	2	0.0				**PHB2**	5	0.0
GANAB	5	0.0	**PLCG2**	2	0.0				**IKBKG**	5	0.0
RBBP4	5	0.0	**VIM**	2	0.0				**ATXN1**	5	0.0
MED26	5	0.0	**BIRC4**	2	0.0				**PDPK1**	5	0.0
PTP4A3	5	0.0	**SMURF1**	2	0.0				**SMN2**	5	0.0
GEMIN4	5	0.0	**STX1A**	2	0.0				**BMPR1B**	5	0.0
VDAC1	5	0.0	**PIAS4**	2	0.0				**SMARCA2**	5	0.0
NKX2-1	5	0.0	**NME2**	2	0.0				**CALD1**	5	0.0
MAP3K1	5	0.0	**CHUK**	2	0.0				**CD79B**	5	0.0
KIF5C	5	0.0	**BARD1**	2	0.0				**APC**	5	0.0
ITGB5	5	0.0	**MDM2**	2	0.0				**ETV6**	5	0.0
STMN1	5	0.0	**HSPA9**	2	0.0				**MED22**	5	0.0
YWHAG	4	0.0	**CCND1**	2	0.0				**CALM1**	5	0.0
MARCKS	4	0.0	**POLE2**	2	0.0				**FLNA**	5	0.0
HMGN1	4	0.0	**BTRC**	2	0.0				**STMN1**	5	0.0
SNIP1	4	0.0	**UBTF**	2	0.0				**RYBP**	5	0.0
MAGI2	4	0.0	**VDAC1**	2	0.0				**HNRNPC**	5	0.0
UBQLN4	4	0.0	**CSNK1D**	2	0.0				**ANXA2**	4	0.0
SKP2	4	0.0	**PHB**	2	0.0				**YBX1**	4	0.0
GPI	4	0.0	**TAF4**	2	0.0				**DUSP12**	4	0.0
GNB2L1	4	0.0	**DYNLL1**	2	0.0				**WASL**	4	0.0
NRIP1	4	0.0	**ELF3**	2	0.0				**CLSTN1**	4	0.0
MAPK10	4	0.0	**MAPK8**	2	0.0				**FGFR1**	4	0.0
CDX2	4	0.0	**TAF10**	2	0.0				**PLD2**	4	0.0
NCOA1	4	0.0	**RBP1**	2	0.0				**PKD1**	4	0.0
KRT18	4	0.0	**TREX1**	2	0.0				**INTS6**	4	0.0
PPP2CA	4	0.0	**TSC22D3**	2	0.0				**GTF2F1**	4	0.0
AURKB	4	0.0	**CALM1**	2	0.0				**BCR**	4	0.0
NUAK1	4	0.0	**PRDX1**	2	0.0				**PRG2**	4	0.0
PLSCR4	4	0.0	**FLNA**	2	0.0				**SH2B2**	4	0.0
RNPS1	4	0.0	**EIF4EBP1**	2	0.0				**BCL2L1**	4	0.0
RAD1	4	0.0	**PPP1R9B**	2	0.0				**ETS1**	4	0.0
HTRA2	4	0.0	**CDK7**	2	0.0				**NCOA1**	4	0.0
PELI3	4	0.0	**TNFAIP3**	2	0.0				**SMC1A**	4	0.0

KRT8	4	0.0	**CIITA**	2	0.0				**MCC**	4	0.0
SERTAD1	4	0.0	**TERT**	2	0.0				**CDKN1C**	4	0.0
XRCC5	4	0.0	**IKBKE**	2	0.0				**MED31**	4	0.0
ELF4	4	0.0	**TRRAP**	2	0.0				**SP3**	4	0.0
CABLES1	4	0.0	**KRTHA3A**	2	0.0				**NCOA3**	4	0.0
ATF5	4	0.0	**RANBP9**	2	0.0				**INSR**	4	0.0
CASP7	4	0.0	**COBRA1**	2	0.0				**SIRT2**	4	0.0
E2F5	4	0.0	**SMARCE1**	2	0.0				**MARK4**	4	0.0
ETV6	4	0.0	**MYBL2**	2	0.0				**CIB1**	4	0.0
APP	4	0.0	**PPIG**	2	0.0				**NEDD9**	4	0.0
TRADD	4	0.0	**ID2**	2	0.0				**TERF2**	4	0.0
PRKCSH	3	0.0	**BATF**	2	0.0				**AKAP8**	4	0.0
BID	3	0.0	**MAPK9**	2	0.0				**PCTK1**	4	0.0
RAC1	3	0.0	**HTATSF1**	2	0.0				**PFTK1**	4	0.0
OGT	3	0.0	**ORC5L**	2	0.0				**ACTA1**	4	0.0
AXIN1	3	0.0	**NFYA**	2	0.0				**GSK3A**	4	0.0
CCNB1	3	0.0	**WEE1**	2	0.0				**DCC**	4	0.0
TOPBP1	3	0.0	**POLR2H**	2	0.0				**ORC6L**	4	0.0
POLI	3	0.0	**RYBP**	2	0.0				**ERCC3**	4	0.0
PTPN1	3	0.0	**E4F1**	2	0.0				**CRKL**	4	0.0
BRAP	3	0.0	**BRE**	2	0.0				**NKX2-1**	4	0.0
KCNK3	3	0.0	**POLE**	2	0.0				**VCP**	4	0.0
ING3	3	0.0	**CLK1**	2	0.0				**E2F3**	4	0.0
NS5A	3	0.0	**HSPH1**	2	0.0				**GAB2**	4	0.0
GTF2H1	3	0.0	**BRF1**	2	0.0				**TRIP10**	4	0.0
NME2	3	0.0	**PRPF40A**	1	-0.1				**CTDP1**	4	0.0
SH3BP2	3	0.0	**YBX1**	1	-0.1				**HDAC6**	4	0.0
NFATC1	3	0.0	**GPHN**	1	-0.1				**BIN1**	4	0.0
WDR8	3	0.0	**NUAK1**	1	-0.1				**PINK1**	3	0.0
SFRS1	3	0.0	**SKP1A**	1	-0.1				**OGT**	3	0.0
KCNK9	3	0.0	**NBN**	1	-0.1				**NTRK1**	3	0.0
HSPA9	3	0.0	**IER2**	1	-0.1				**MITF**	3	0.0
NR4A1	3	0.0	**SMN1**	1	-0.1				**PTPN18**	3	0.0
BTRC	3	0.0	**KDR**	1	-0.1				**SMARCC2**	3	0.0
FOS	3	0.0	**CLSPN**	1	-0.1				**DAB2**	3	0.0
IQGAP1	3	0.0	**COPB1**	1	-0.1				**PTPRE**	3	0.0
CAMK2A	3	0.0	**CLSTN1**	1	-0.1				**PTK2B**	3	0.0
PDE6D	3	0.0	**JUND**	1	-0.1				**TELO2**	3	0.0
EEF1E1	3	0.0	**PHB2**	1	-0.1				**PPP5C**	3	0.0
SYN1	3	0.0	**GANAB**	1	-0.1				**CLN5**	3	0.0
SPTBN1	3	0.0	**RARA**	1	-0.1				**NEDD4**	3	0.0
EZR	3	0.0	**POLI**	1	-0.1				**FHOD1**	3	0.0
DYNC1H1	3	0.0	**RAD51**	1	-0.1				**DNM1**	3	0.0
KCNK15	3	0.0	**CD4**	1	-0.1				**SETDB1**	3	0.0
CDC6	3	0.0	**ING3**	1	-0.1				**CAMK2A**	3	0.0
PPARG	3	0.0	**SH3KBP1**	1	-0.1				**PTHLH**	3	0.0
JAG1	3	0.0	**TLK1**	1	-0.1				**PPP2R1A**	3	0.0
FBL	3	0.0	**CUL7**	1	-0.1				**ACVR1**	3	0.0
TIAM1	3	0.0	**HMGN1**	1	-0.1				**COIL**	3	0.0
RUNX2	3	0.0	**ADRA1B**	1	-0.1				**TSC2**	3	0.0
STUB1	3	0.0	**SNCAIP**	1	-0.1				**RUNX1**	3	0.0
NCOA3	3	0.0	**NONO**	1	-0.1				**CFTR**	3	0.0
MTHFD1	3	0.0	**GTF2H1**	1	-0.1				**TFAP2A**	3	0.0
CDK6	3	0.0	**SET**	1	-0.1				**PPP1R12A**	3	0.0
CSK	3	0.0	**PRKAR1A**	1	-0.1				**ATP1A1**	3	0.0
SMAD7	3	0.0	**RUNX3**	1	-0.1				**YWHAZ**	3	0.0
ZBTB16	3	0.0	**NASP**	1	-0.1				**KLKB1**	3	0.0
MAPK8IP3	3	0.0	**MAF**	1	-0.1				**PPP1R1B**	3	0.0
CSNK2B	3	0.0	**NFATC1**	1	-0.1				**CDKN2D**	3	0.0
CUX1	3	0.0	**POU5F1**	1	-0.1				**ILK**	3	0.0
PCTK1	3	0.0	**GNAS**	1	-0.1				**TGIF1**	3	0.0
TGFBR1	3	0.0	**NEDD4**	1	-0.1				**CLSPN**	3	0.0
LIG4	3	0.0	**MAP2K1**	1	-0.1				**VASP**	3	0.0
GSK3A	3	0.0	**NFKB1**	1	-0.1				**ZYX**	3	0.0
REM1	3	0.0	**ATXN7**	1	-0.1				**PELI3**	3	0.0
CASP4	3	0.0	**IKBKB**	1	-0.1				**WAS**	3	0.0
APEX1	3	0.0	**GSPT2**	1	-0.1				**ARRB1**	3	0.0
MAPK8IP2	3	0.0	**ELF4**	1	-0.1				**GIPC1**	3	0.0
GNA13	3	0.0	**MED26**	1	-0.1				**ITK**	3	0.0
VAV1	3	0.0	**GTF3C3**	1	-0.1				**IFNAR2**	3	0.0

PRKCB1	3	0.0	**ORC4L**	1	-0.1				**ING1**	3	0.0
EXOS	3	0.0	**RBX1**	1	-0.1				**SUPT16H**	3	0.0
TOP1	3	0.0	**NR2E3**	1	-0.1				**TREX1**	3	0.0
MYB	3	0.0	**PELO**	1	-0.1				**BRAF**	3	0.0
ANXA2	2	0.0	**CREB1**	1	-0.1				**GPS2**	3	0.0
PRKCE	2	0.0	**PPP2R3B**	1	-0.1				**BATF**	3	0.0
DLG1	2	0.0	**GRB2**	1	-0.1				**EEF1A1**	3	0.0
PINK1	2	0.0	**CDK4**	1	-0.1				**SMARCD3**	2	0.0
ROCK1	2	0.0	**TERF1**	1	-0.1				**ZAP70**	2	0.0
DDEF2	2	0.0	**FKBP3**	1	-0.1				**POLR2G**	2	0.0
KLF1	2	0.0	**ING1**	1	-0.1				**NBN**	2	0.0
HNRPD	2	0.0	**ASF1B**	1	-0.1				**EIF2AK2**	2	0.0
NTRK1	2	0.0	**RBBP8**	1	-0.1				**RAC1**	2	0.0
MITF	2	0.0	**SPTBN1**	1	-0.1				**PRKAR2B**	2	0.0
EXOC4	2	0.0	**SND1**	1	-0.1				**PTEN**	2	0.0
LMNB1	2	0.0	**IRS1**	1	-0.1				**U2AF2**	2	0.0
KIAA1446	2	0.0	**RNASEH2B**	1	-0.1				**MLLT7**	2	0.0
CDK9	2	0.0	**ETV1**	1	-0.1				**UBA1**	2	0.0
RXRA	2	0.0	**KIAA1967**	1	-0.1				**GTF2H1**	2	0.0
MAP3K5	2	0.0	**ETS2**	1	-0.1				**BIRC4**	2	0.0
NASP	2	0.0	**NFE2L1**	1	-0.1				**EBNA1**	2	0.0
NOS1	2	0.0	**AP3B2**	1	-0.1				**SLK**	2	0.0
PRMT5	2	0.0	**GSPT1**	1	-0.1				**PFKFB2**	2	0.0
KPNA2	2	0.0	**BAX**	1	-0.1				**SNIP1**	2	0.0
PRKG1	2	0.0	**GPS2**	1	-0.1				**SQSTM1**	2	0.0
GNAS	2	0.0	**JAG1**	1	-0.1				**BIRC5**	2	0.0
NPHP1	2	0.0	**TRIP10**	1	-0.1				**IKBKB**	2	0.0
GTF2F1	2	0.0	**HIST1H1A**	1	-0.1				**ARHGAP1**	2	0.0
PCYT1A	2	0.0	**TGFA**	1	-0.1				**PCYT1A**	2	0.0
BCR	2	0.0	**SFRS3**	1	-0.1				**PURA**	2	0.0
CASP10	2	0.0	**DBF4**	1	-0.1				**HAND1**	2	0.0
PELO	2	0.0	**EGR1**	1	-0.1				**FOS**	2	0.0
FAS	2	0.0	**CREM**	1	-0.1				**TOM1L1**	2	0.0
HAND1	2	0.0	**EEF1A1**	1	-0.1				**CRIP2**	2	0.0
TUBB	2	0.0	**TIAM1**	1	-0.1				**H3F3B**	2	0.0
HOOK2	2	0.0	**NCKIPSD**	1	-0.1				**TAF11**	2	0.0
STAT5B	2	0.0	**PKN1**	1	-0.1				**HSP90AB1**	2	0.0
PIK3CB	2	0.0	**TFAP2A**	1	-0.1				**EIF4EBP1**	2	0.0
SUPT5H	2	0.0	**BIN1**	1	-0.1				**PPARG**	2	0.0
TCERG1	2	0.0	**HMGB1**	1	-0.1				**CIITA**	2	0.0
MEF2A	2	0.0	**PARP1**	1	-0.1				**TRRAP**	2	0.0
FEN1	2	0.0	**NR3C1**	1	-0.1				**ADCY6**	2	0.0
SND1	2	0.0	**TOP1**	1	-0.1				**HCFC1**	2	0.0
APLP2	2	0.0	**NCKAP1**	1	-0.1				**SORBS2**	2	0.0
SDC2	2	0.0	**THRA**	1	-0.1				**INPP5D**	2	0.0
ETS2	2	0.0	**HUWE1**	1	-0.1				**HSPH1**	2	0.0
NFE2L1	2	0.0							**HDAC3**	2	0.0
ARPC1B	2	0.0							**IL7R**	2	0.0
MARK3	2	0.0							**MAP4K1**	2	0.0
HIST1H1A	2	0.0							**IL16**	2	0.0
TNFRSF14	2	0.0							**PITPNA**	2	0.0
RGS19	2	0.0							**RNPS1**	2	0.0
TRIM37	2	0.0							**MAP1B**	2	0.0
FBXW7	2	0.0							**HIST4H4**	2	0.0
KLKB1	2	0.0							**RANBP10**	2	0.0
POLE	2	0.0							**MORF4L2**	2	0.0
GFAP	2	0.0							**ACP1**	2	0.0
MAP4K1	2	0.0							**SYNJ1**	2	0.0
ILK	2	0.0							**BRD2**	2	0.0
MAP1B	2	0.0							**ZBTB16**	2	0.0
TPT1	2	0.0							**VIM**	2	0.0
CENPJ	2	0.0							**NONO**	2	0.0
IER3	2	0.0							**RBBP4**	2	0.0
NGFRAP1	2	0.0							**CDKN2C**	2	0.0
CIB1	2	0.0							**CHUK**	2	0.0
NEDD9	2	0.0							**RUVBL1**	2	0.0
NONO	2	0.0							**XRCC5**	2	0.0
NOLC1	2	0.0							**PAK3**	2	0.0
CASP1	2	0.0							**ELF4**	2	0.0
PPFIBP1	2	0.0							**MED26**	2	0.0

EIF3K	2	0.0							**PCGF2**	2	0.0
NCF1	2	0.0							**GEMIN4**	2	0.0
NFKB1	2	0.0							**AATF**	2	0.0
HSPA1A	2	0.0							**FOXO3**	2	0.0
IRS2	2	0.0							**GAPDH**	2	0.0
PSEN1	2	0.0							**PSEN1**	2	0.0
ING1	2	0.0							**STMN2**	2	0.0
TP53BP1	2	0.0							**PARK2**	2	0.0
ERCC3	2	0.0							**PLAUR**	2	0.0
ATP6V1E1	2	0.0							**CEBPE**	2	0.0
STMN2	2	0.0							**MAP3K1**	2	0.0
ETV1	2	0.0							**ARID2**	2	0.0
NF2	2	0.0							**AP3B2**	2	0.0
TREX1	2	0.0							**CTTN**	2	0.0
WWOX	2	0.0							**TRADD**	2	0.0
CALM1	2	0.0							**RPS6KA2**	2	0.0
CEBPE	2	0.0							**PDE3B**	2	0.0
VCP	2	0.0							**SYP**	2	0.0
AP3B2	2	0.0							**TOP1**	2	0.0
GORASP1	2	0.0							**PTPRC**	2	0.0
MCL1	2	0.0							**MYB**	2	0.0
CAMK2G	2	0.0							**SKP1A**	1	-0.1
TP53BP2	2	0.0							**KLF1**	1	-0.1
BATF	2	0.0							**HNRPD**	1	-0.1
FGFBP1	2	0.0							**PNKP**	1	-0.1
PTPRC	2	0.0							**DAF**	1	-0.1
YBX1	1	-0.1							**EXOC4**	1	-0.1
ZAP70	1	-0.1							**USF2**	1	-0.1
POLR2G	1	-0.1							**CSNK1E**	1	-0.1
PSTPIP1	1	-0.1							**YEATS4**	1	-0.1
SKP1A	1	-0.1							**NR2F1**	1	-0.1
SOS1	1	-0.1							**RPS6KA5**	1	-0.1
SRCAP	1	-0.1							**MAPKAPK2**	1	-0.1
TUBA4A	1	-0.1							**STK6**	1	-0.1
SMARCC2	1	-0.1							**RFC3**	1	-0.1
SMARCC1	1	-0.1							**AFAP1L2**	1	-0.1
USF2	1	-0.1							**DIAPH2**	1	-0.1
MLLT7	1	-0.1							**TBK1**	1	-0.1
BAK1	1	-0.1							**BAZ1B**	1	-0.1
BBC3	1	-0.1							**TXK**	1	-0.1
PLD2	1	-0.1							**NFATC1**	1	-0.1
ARF6	1	-0.1							**SIC1**	1	-0.1
PLCG2	1	-0.1							**DNMT1**	1	-0.1
BIRC4	1	-0.1							**POLR1B**	1	-0.1
STK6	1	-0.1							**PLK3**	1	-0.1
RFC3	1	-0.1							**SUV39H1**	1	-0.1
STX1A	1	-0.1							**PAX6**	1	-0.1
GDNF	1	-0.1							**MKNK1**	1	-0.1
AFAP1L2	1	-0.1							**PAFAH1B1**	1	-0.1
TGM2	1	-0.1							**CCNB2**	1	-0.1
RUNX3	1	-0.1							**RASGRF1**	1	-0.1
SP100	1	-0.1							**FADD**	1	-0.1
HRK	1	-0.1							**ERBB2**	1	-0.1
DNMT1	1	-0.1							**BTRC**	1	-0.1
AKAP1	1	-0.1							**IQGAP1**	1	-0.1
PPP3R1	1	-0.1							**YWHAQ**	1	-0.1
PPM1B	1	-0.1							**XPA**	1	-0.1
SUV39H1	1	-0.1							**KIAA1377**	1	-0.1
PPP3CA	1	-0.1							**MAP3K14**	1	-0.1
MED17	1	-0.1							**PPP1R9A**	1	-0.1
TUBA8	1	-0.1							**SKI**	1	-0.1
ARHGAP1	1	-0.1							**AP1B1**	1	-0.1
PAFAH1B1	1	-0.1							**SUPT5H**	1	-0.1
PLEC1	1	-0.1							**TRPV4**	1	-0.1
TAF1	1	-0.1							**KCNH2**	1	-0.1
FOXM1	1	-0.1							**CAMK2D**	1	-0.1
PF4	1	-0.1							**SPTBN1**	1	-0.1
DAPK3	1	-0.1							**SND1**	1	-0.1
PTK2	1	-0.1							**MED8**	1	-0.1
XPO1	1	-0.1							**ACTC1**	1	-0.1

SETDB1	1	-0.1							**DYNC1H1**	1	-0.1
XPA	1	-0.1							**PPP1R9B**	1	-0.1
KIAA1377	1	-0.1							**BAG1**	1	-0.1
PTHLH	1	-0.1							**TFAP2B**	1	-0.1
CCNT1	1	-0.1							**DNM2**	1	-0.1
ERBB2IP	1	-0.1							**MED21**	1	-0.1
KLF5	1	-0.1							**BRD8**	1	-0.1
KCNH2	1	-0.1							**MRE11A**	1	-0.1
RBBP8	1	-0.1							**STAU1**	1	-0.1
LUC7L2	1	-0.1							**RGS19**	1	-0.1
CAMK2D	1	-0.1							**HTATSF1**	1	-0.1
RNASEH2B	1	-0.1							**ZEB2**	1	-0.1
TUBA3C	1	-0.1							**NCKIPSD**	1	-0.1
TSG101	1	-0.1							**FBXW7**	1	-0.1
RBBP7	1	-0.1							**MED15**	1	-0.1
TSC22D3	1	-0.1							**HEXIM1**	1	-0.1
APOB	1	-0.1							**E2F2**	1	-0.1
HSP90AB1	1	-0.1							**BRF1**	1	-0.1
ZRSR2	1	-0.1							**HUWE1**	1	-0.1
BCAS1	1	-0.1							**BTK**	1	-0.1
CDK7	1	-0.1							**AURKB**	1	-0.1
BAG1	1	-0.1							**FAF1**	1	-0.1
TFAP2B	1	-0.1							**YWHAH**	1	-0.1
CFTR	1	-0.1							**EWSR1**	1	-0.1
STAT5A	1	-0.1							**COPB1**	1	-0.1
DBF4	1	-0.1							**JUND**	1	-0.1
EGR1	1	-0.1							**SUB1**	1	-0.1
MAP3K4	1	-0.1							**SMARCA5**	1	-0.1
CYLD	1	-0.1							**SH3KBP1**	1	-0.1
POLR2H	1	-0.1							**HTRA2**	1	-0.1
TUBA1B	1	-0.1							**SMAD7**	1	-0.1
CDR2	1	-0.1							**TANK**	1	-0.1
MTA1	1	-0.1							**MYCBP**	1	-0.1
ATP1A1	1	-0.1							**FHIT**	1	-0.1
PIM1	1	-0.1							**MPP1**	1	-0.1
HUWE1	1	-0.1							**APAF1**	1	-0.1
BRF1	1	-0.1							**GRAP**	1	-0.1
HDAC3	1	-0.1							**NMT1**	1	-0.1
BTK	1	-0.1							**YAP1**	1	-0.1
PPP1CC	1	-0.1							**ARR3**	1	-0.1
PAXIP1	1	-0.1							**BHLHB2**	1	-0.1
UIMC1	1	-0.1							**CGN**	1	-0.1
DISC1	1	-0.1							**TPM1**	1	-0.1
LEF1	1	-0.1							**MAPKBP1**	1	-0.1
DOK4	1	-0.1							**PSMC3**	1	-0.1
SRFBP1	1	-0.1							**ORC4L**	1	-0.1
PACSIN3	1	-0.1							**E2F4**	1	-0.1
MORF4L2	1	-0.1							**NSMAF**	1	-0.1
ASAP1	1	-0.1							**NUMA1**	1	-0.1
SYNJ1	1	-0.1							**SORBS3**	1	-0.1
TCF7L2	1	-0.1							**DMTF1**	1	-0.1
JAK1	1	-0.1							**SFN**	1	-0.1
ADAM17	1	-0.1							**ACTN1**	1	-0.1
SET	1	-0.1							**PHB**	1	-0.1
HIPK2	1	-0.1							**ITGB2**	1	-0.1
RAD52	1	-0.1							**POU2F1**	1	-0.1
CCND2	1	-0.1							**PRKA4**	1	-0.1
FHIT	1	-0.1							**HIST3H2BB**	1	-0.1
MLXIPL	1	-0.1							**EEF2K**	1	-0.1
GCN5L2	1	-0.1							**CASP2**	1	-0.1
MAPKBP1	1	-0.1							**PSEN2**	1	-0.1
TDRD7	1	-0.1							**RANBP2**	1	-0.1
SMARCA2	1	-0.1							**BIRC2**	1	-0.1
BMX	1	-0.1							**RBP1**	1	-0.1
CALD1	1	-0.1							**SLC9A3R2**	1	-0.1
RRAS	1	-0.1							**WWOX**	1	-0.1
RPL31	1	-0.1							**EPHB2**	1	-0.1
PCGF2	1	-0.1							**CD3E**	1	-0.1
CDC20	1	-0.1							**ACHE**	1	-0.1
POU2F1	1	-0.1							**PTPN13**	1	-0.1

GNA12	1	-0.1							**GMEB1**	1	-0.1
MED22	1	-0.1							**FOXO1**	1	-0.1
EEF2K	1	-0.1							**TESK1**	1	-0.1
HOXB7	1	-0.1							**FBXO7**	1	-0.1
CEP57	1	-0.1							**CCND3**	1	-0.1
BRAF	1	-0.1							**SMYD2**	1	-0.1
PAX5	1	-0.1							**MED30**	1	-0.1
LASP1	1	-0.1							**ORC5L**	1	-0.1
BAX	1	-0.1							**LIMK2**	1	-0.1
PTPN13	1	-0.1							**DCLRE1C**	1	-0.1
HGS	1	-0.1							**TNNT1**	1	-0.1
ACTN2	1	-0.1									
RBAK	1	-0.1									
LNX1	1	-0.1									
CASP8AP2	1	-0.1									
RYBP	1	-0.1									
ITGB3BP	1	-0.1									
BIN1	1	-0.1									

Table S6: Occurrences of nodes in shortest path networks.

Table S6 gives the complete list of molecules and the number of times each molecules occurred in shortest paths networks along with the normalized z-score for each molecule.

Table S8

Classification of nodes according to their presence in different phase specific modules.

Functional groups	Molecules unique to G1	Common molecules between G1 and G1S	Molecules Unique to G1S		Common molecules between G1S and S	Molecules unique to S
Signaling intermediates	YWHAQ BAD HRAS CRK LCK PTK2B MAPK8 PTPN12 SYNGAP1 ASAP1 PRG2 ARHGEF7	ADRB2 AKT1 CDC25B PDGFRB GRB2 CSNK2A1 ERBB2 MST1R PDE6G PDPK1 PTPN18 SHB SHC SRC CTNNB1 BCAR1	RGS16 CHEK2 WASL GNB2L1 PRKCD MNAT1 MAPK14 CDKN1B YWHAB PELP1 PRKDC MAPK3 MAP2K1 MDM2	ABL1 CDK5 EGFR JAK1 LYN PTPN2 PTPN6 PTPRE RPS6KA1 CASP9 PIAS3 JAK2 NBN	CDK2	
Transcription Regulators		CREBBP E2F1 ESR1 FOXO1 FOXO3 IKBKB MYC STAT3 TRP53 TSC2	SP1 ELK1 EP300 GTF2I JUN MYB STAT1 STAT5B NCOA3	TRIP4 TRP73 STAT5A CITED1 SMAD2 SMARCA4 SMAD3 E6	BRCA1 E7	TAF1
DNA replication factors		SKP2 SP3	YTHDC1 MCM7		RIS2	
Other Cell Cycle Regulators		HSP90AA1	CCNT1 YTHDC1	RB1 RBP1	CCNA2 RBL1	RBL2 HDAC1

LEGENDS FOR SUPPLEMENTARY TABLES

Table S1: siRNA screen results for targeted kinases and phosphatases.

Table S1 gives the complete details of the primary and validation screens of all kinases and phosphatases. This includes siRNA target sequences, the raw value for cell cycle distribution obtained from FACS, and the frequency of dead cell populations. Data for each of the replicates, with their normalized values, are provided along with the final mean of two replicates used for hit selection. The table gives additional information about ontology of the molecules and variants.

Table S2: Gene expression status of the validated hits.

Table S2 provides the expression status of the final validated hits in CH1 cells. Raw expression values for the 43 hits identified by our RNAi screen are listed with corresponding probe sequence. Microarray data are available in the ArrayExpression Database (Accession No. E-MTAB-82).

Table S5: High confidence network used for graph theory analysis.

The complete interaction file compiled by merging and filtering the different databases have been provided in table S5 as a two column file.

Table S7: Network file used as SNAVI background.

The flat file used for detection of motifs using SNAVI is provided in table S7 with the complete information regarding the interactors, the type of interaction, biochemical process and the PMID providing evidences for the interaction.

SUPPLEMENTARY EXPERIMENTAL PROCEDURES.

Cell Lines and Cell Culture Medium

Murine B cell Lymphoma CH1 (TIB-221) cells were cultured in RPMI 1640 (Invitrogen) medium with 2mM L-glutamine adjusted to contain 1.5 g/L Na bicarbonate, 4.5 g/L glucose, 10 mM HEPES, 0.05 mM 2-mercaptoethanol (90%) ,1.0 mM Na pyruvate and 10% fetal calf serum.

Human cell lines Raji, Jurkat, HL60, U937 and THP1 were cultured in RPMI 1640 medium with 2mM L-glutamine adjusted to contain 1.5g/L Na bicarbonate,4.5g/L glucose,10 mM HEPES, and 10% fetal calf serum.

Human Burkitts Lymphoma Namalwa was cultured in RPMI 1640 medium with 2mM L-glutamine adjusted to contain 1.5g/L Na bicarbonate,4.5g/L glucose,10 mM HEPES, and 1.0 mM Na pyruvate and 10% fetal calf serum.

Human cell lines A549, HeLa, HepG2, HEK293, U2OS, AW8507, MCF7 and Huh7 and were maintained in DMEM (Dulbecco's Modified Eagle Medium, Invitrogen) supplemented with 10% FCS. All cell lines were cultures at 37^0C and 5% CO2.

siRNA libraries

The primary siRNA screens were performed using siRNA libraries targeting mouse Kinases (Mouse Kinase siRNA SET V1.0) and Phosphatases (Mouse Phosphatase siRNA SET V1.0) containing 2 siRNA duplexes for each target gene (Qiagen).The siRNAs were designed using the innovative HiPerformance siRNA design algorithm. A pool of the 2 siRNAs was used and a total of 758 Kinases and 294 phosphatases were screened.

The Validation screen for the shortlisted Kinase hits was performed using pools of 3 individual siRNA duplexes against each gene target from the MISSION siRNA Mouse

Kinase Panel (Sigma).The screen was performed similar to the primary screen. For Validation of Phosphatases, siGENOME (Dhramacon) smartpool siRNAs containing 4 siRNAs per target gene were used.

Standardization of the screening procedure:

(i) ***No. of Cells Plated/ Well***

Experiments were done to determine the optimum number of cells to be used per well for transfection and subsequently for cell cycle analysis. CH1 cells were seeded at varying numbers ranging from 10,000/well to 50,000/well and transfected with GFP-specific siRNA. Subsequently, cell viability was determined using trypan blue exclusion at 24, 48, and 72 hours. A seed density of 20,000 cells/well was found to be optimal with a cell viability that was consistently >85%.

(ii) ***siRNA Transfection Conditions***

Transfection efficiency: To ensure efficient transfection Alexa 488 labelled siRNA was used to transfect CH1 cells. 20,000 cells were plated in a 96-well plate and transfected using HiPerfect transfection reagent. Transfection was carried out as per the manufacturer's protocol. The efficiency was monitored at up to 72 hours post transfection using confocal microscopy and was found to be >98%.

Optimal siRNA concentration and the kinetics of Knockdown: To determine optimal knockdown conditions siRNAs against six representative proteins were chosen. Using the optimised cell number (20,000/well) experiments were set up with different concentrations of siRNA ranging from 50 to 400nM using HiPerfect transfection reagent as per manufacturers protocol. The effect of different siRNA knockdowns on protein level was determined by Western blot analysis in cell lysates obtained at 24, 36, 48, 72 and 96h after transfection. Across experiments the siRNA concentration of 200nM was found to be optimal, giving a

knockdown of between 70-80%, which was retained up to 96h post transfection. The western blots for two representative molecules BTK and PLK1, along with those for three validated screen targets are shown in Figure S1B. The relatively higher concentration of siRNA required is likely due to the fact that these cells grow as a suspension.

siRNA Screen

The mouse Kinase and phosphatase libraries (Qiagen) containing 2 siRNAs per target gene were obtained in a 96 well format. The siRNAs were diluted to a working concentration of 10μM. CH1 mouse B cell lymphoma cells were transfected with the pool of 2 siRNA duplexes per target gene, using HiPerfect transfection reagent as per the manufacturer's protocol for transfection of suspension cell lines (Qiagen). Briefly, 20,000 cells of mouse lymphoma cell line CH1 in 25uL of RPMI were seeded into each well of a flat bottom 96 well plate. The cells were incubated at 37^0C and 5% CO_2 for 30 minutes. Meanwhile, 25uL (per well) of transfection mix, containing RPMI medium and a 1:1 volume ratio of siRNA and transfection reagent Hiperfect i.e. 200nM (3ul) siRNA and 3ul HiPerfect were prepared in parallel U-bottom 96 well plates. To each well in the plate containing cells, 25ul of transfection mix was added. The mixture was pipetted a few times to ensure proper mixing of transfection complexes with the cells. The plates were incubated at 37^0C and 5% CO_2. At 6 hours post transfection the volume of each well was made up to 150 uL with complete medium (RPM1 with 10% FCS, 1mM sodium Pyruvate, Bme). At 24 and 48 hours post transfection the medium of the plate was replaced with fresh complete medium. Our transfection conditions ensured that >98% of the cells were transfected with the siRNA. Further, by using siRNA pools against a representative set of cellular kinases we determined that specific depletion was evident by 36 h after transfection, and that this attained maximal levels by 48h. Depleted protein levels then persisted up to 96h of the culture (Figure S1B).

Since during standardization experiments the target protein levels were found to be the lowest at 48 hours post transfection, the cell cycle analysis was performed at 72 hours (which is 24 hours after the point at which protein levels are minimum). Each plate had 5 negative control wells which included cells treated with scrambled siRNA (2 wells), GFP siRNA (2 wells) and 1 well contained mock transfected cells (i.e. only HiPerfect). All the screens were performed in duplicates.

Propidium Iodide staining and sample acquisition

For propidium iodide staining and DNA content analysis the cells were centrifuged in the 96 well plates using a plate rotor and the medium was aspirated. The cells were stained for 30 minutes at 4^0C with 150 uL propidium iodide staining solution containing 0.1mg/mL Propidium Iodide (Sigma), 3ul/mL TritonX -100 (Sigma),1 mg/mL sodium citrate (Sigma) and 20ug/mL RNase (Sigma). Plates which were not acquired immediately were kept at 4^0C. The samples were acquired in a 96-well plate format using an automated BD FACSCalibur HTS or High Throughput Sampler (Beckton Dickinson, FACSCalibur).

Primary and secondary screen data analysis and hit selection

The data obtained was analysed using FlowJo software and the DNA histograms obtained were analysed to quantitate the subG1, G1, S and G2 populations. During data analysis we observed minor shifts in G1 and G2 peak positions and widths across cell cycle histograms. This prevented a reliable quantification and comparison of S and G2 phases of the cell cycle using automated platforms such as those available with FlowJo. The cell cycle histograms were therefore analysed using manual gating of the sub-G1, G1, S and G2 phases. The G1, S and G2 phases were analysed after gating out the subG1 population such that their quantified values represent percentages of the total live cell population.

For each plate the gates were defined for the negative control samples and the same gates were copied to the other histograms and used for analysis. Although with respect to the control sample there were some well-dependent (instrument based) and sample dependent shifts in peaks of some samples in each plate. To increase precision of analysis small adjustments in the gates of individual peaks of each sample allowed reliable quantification of cell cycle phases. The same procedure was used for the analysis of the data obtained from the second screen.

To allow the comparison of data sets from different plates the data was normalized by calculating and representing each quantified parameter sub G1, G1, S and G2 populations into Z scores (also called normal scores). Each Z-score is a dimensionless quantity which depicts the deviation of the data point from the mean of the negative controls in units of the standard deviations of the negative control. The Z scores were calculated for each parameter with respect to the mean and standard deviations of the 5 negative controls of its respective plate. Each Z score was calculated as follows:

$$\text{Z score}=(x-\mu)/\sigma$$

Where x is the G1/S/G2 population to be standardised, μ is the plate mean/mean of controls and σ is the standard deviation of the plate/plate controls. Both the screens were performed in duplicates, therefore for each siRNA knockdown there were two Z scores. The Z scores were obtained for each duplicate and the mean was calculated. For the first screen a z score cut off of $Z > \pm 2.5$ was chosen and 83 kinases and 22 phosphatases were shortlisted as our primary hits.

The molecules shortlisted were screened in the second screen using new siRNAs obtained from an alternative source and having sequences which were different from those used in the

primary screen. All siRNAs which resulted in a Z score cut off of ± 2.0 were shortlisted as the final hits. The final list of hits included 38 kinases and 5 phosphatases as the final hits.

An analysis of the distribution of scores obtained across the entire screen yielded a normal distribution profile with a very low 'skewness' value (Figure S1A). Further, a comparison of *z*-scores between the replicates revealed that the potency of identified targets remained largely comparable (Figure S2). Also, both intra- and inter-plate variations for the control wells were low with a percent standard deviation of the median value of <10%. In order to assess the over all reproducibility of the screen we calculated the z-factor with PLK1 as positive control. This resulted in a z-factor of 0.56 which is considered to represent an overall high quality for the assay conditions. These collective results, therefore, confirm the robustness, reproducibility, and sensitivity of our primary screen. (Figure S1, S2).

Population Doubling Time Experiments (PDTs).

To assess the effects of siRNA knockdown on cell cycle dynamics and population doubling time, the following experiments were carried out with the validated siRNA hits. The siRNA transfections were set up in duplicates and carried out in a 96-well plate format as described above. At 48 hours post knockdown (point of maximum knockdown) the first population doubling sample was taken and the cells were counted using trypan blue exclusion to give the "day 0" counts. Cells were counted similarly at 72 hours and 96 hours to give the "day 1" and "day 2" counts respectively. Here it should be emphasized that the loss of function due to siRNA knockdown is observed up to 96 hours (Figure S1B), which is within the recommended time frame for siRNA mediated transient knockdown experiments [1]. Population doubling times (PDTs) were calculated using the formula (log 2/log N) hr, where N is final cell count/initial cell count (N_f/N_i) and hr is time (in hours) between initial and final

cell count. The population counts were used to plot population growth curves, and also to calculate the PDTs.

Calculation of Residence Times

Using the population doubling times and the cell cycle histograms, the average residence times (RT) of cells in different cell cycle phases were calculated as described earlier [2]. The residence time in a particular phase G1/S/G2 (hrs) = % cells in G1/S/G1 x PDT (hrs). A table indicating the population doubling times and respective residence times is given in Table S3.

PDTs were determined for both mock-silenced, as well as 'hit'-silenced CH1 cells. The doubling time for mock-silenced CH1 cells was 26 hrs (SD ±3 hours), and the individual phase-specific RTs were calculated to be G1-8.41 (SD ±1.5), S-13.48 (SD ±1), G2-4.11 (SD ±0.5). The results discussed in the text clearly indicate that each siRNA shortlisted as a 'hit' affected one or more cell cycle phase in terms of RT extensions. Since our interest was to understand regulatory networks involved in G1 and S phase control, we grouped the hits based on residence times alone. Many patterns of perturbation in RT were observed in the resulting data. The residence times calculated are a reflection of the Z scores. A normalization procedure was carried out to negate the plate to plate fluctuations of control cell percentages and allow comparison between the different PDTs.

Western blot analysis

Western blot analysis was done to assess efficiency of siRNA knockdown. At appropriate times after knockdown i.e 24 hrs, 48 hrs, 72 hrs and 96hrs, aliquots of cells were collected, centrifuged, and the cell pellets stored in liquid nitrogen. Just prior to electrophoresis, cells were lysed in lysis buffer (20mM HEPES, 10mM NaCl, 1.5nM MgCl2, 0.2mM EDTA, 0.5% Triton X-100, 0.5mM DTT, 1mM sodium orthovanadate, 1mM NaF, and a cocktail of protease inhibitors) followed by removal of the nuclear material and other debris through

centrifugation. The detergent-soluble proteins were then resolved by SDS–PAGE. Specific proteins and phosphoproteins were detected by Western blot using appropriate antibodies. Blots were scanned and analyzed on an Odyssey Infrared Imaging System.

Rationale for assigning cell cycle phase specific source and targets.

We identified thirty eight kinases and five phosphatases as hits from our siRNA screen (Figure 1B, 1D). Kinases and phosphatases are generally considered as molecules involved in signaling mechanisms. We wanted to classify the siRNA screen hits as signaling molecular sources affecting cell cycle. Initially we could classify the hits as molecules causing extension or no extension in cell cycle duration from the population doubling time data (Figure 1D). Then we further classified these hits as affecting a particular phase based only on extent of the increase in the residence time of a particular phase but not reduction in the residence time of a particular phase to simplify further data analysis. These hits must affect the cell cycle machinery either directly or indirectly to induce such drastic changes in the residence times of each cell cycle phases.

We defined 12 molecules as sources for causing G1 extension, 9 for S phase extension, 4 for G2 phase extension on the basis of their residence time (Table S3). We further classified 15 molecules as both G1S phase specific sources since they affected both the phases to an equal extent. Similarly we had 1 molecule in G1G2 and 2 in SG2 sources. By this process we defined sources for cell cycle regulation based on our siRNA screen results and population doubling experiments. We have included PPV scores as the ratio of confirmed predictions versus the total number of predictions for a given RNAi hit (Table S3). For this we pooled the individual phases to broadly define involvement of the siRNA ‘hits’ in the cell cycle and/or proliferation. Since it was not trivial to define the total number of predictions for a molecule available in the literature, we used Gene Ontology for the scoring purposes wherein GO terms – pertaining to biological processes –

for the hits were scanned and those classes under cell cycle/proliferation (e.g. G1 regulation, mitosis etc.) were scored as a confirmed prediction. On the other hand, the total number of GO classes for the given molecule was considered as the total predictions.

By extensive literature curation on cell cycle we shortlisted molecules involved directly in the regulation of cell cycle (Table S4). The target list consisted of 93 molecules grouped into 3 classes, those which are involved in regulating the G1 phase, the S phase and the G2 phase. Many cell cycle regulators are known to play a role in G1 to S phase progression or in both G1 and S phase regulation. These have been listed as possible G1 as well as S phase targets. These molecules include core cell cycle regulators such as cyclins and CDKs, transcription factors, molecules involved in DNA replication and kinases/phosphatases which are known to play a role in cell cycle. Some of the molecules shortlisted as targets were also screened in the siRNA libraries and were shortlisted as the screen and PDT hits. These molecules may therefore appear as sources, targets and possible intermediates of the shortest paths during network analysis.

This set of 93 molecules was considered as molecular targets controlling cell cycle. Since we wished to study the phase specific regulation of cell cycle we categorized these molecules as $G1_{targets}$ (51), $S_{targets}$ (53) and $G2_{targets}$ (29) based on their involvement in regulation of a particular phase. We combined both $G1_{targets}$ and $S_{targets}$ molecules list to get $G1S_{target}$ molecules. From the experimental and literature information we could define set of source-target relationships for phase specific cell cycle regulation.

Network analysis methods

***Construction of mammalian protein-protein interaction database*:** We downloaded seven different mammalian protein-protein interaction (PPI) databases (i.e., reported to be present in rat/mouse/human) from the following sources, BIND [3], BioGRID [4], IntAct [5], MINT

[6], HPRD [7], NetworKIN [8] and Reactome [9]. The consolidation of the different databases was achieved by merging human/mouse/rat gene symbols using the xml version of UniprotKB downloaded from http://www.uniprot.org/downloads to yield a single PPI database with ~12000 nodes and ~50000 edges. Since most of the experimental work has been performed in other model systems it was imperative for us to use the collated information to obtain a more comprehensive core network. Here it must be mentioned that we used information from only higher organisms and have omitted interactions from Yeast, *E.coli* etc. In order to incorporate all high confidence experimental/biochemical interactions, we incorporated a filter criterion to prune out those interactions (edges) that were not reported by at least two different experimental methods. We also removed interactions predicted purely by *in silico* and high throughput methods. This yielded us a high confidence PPI network of ~5200 nodes and ~12000 edges essentially including all known direct experimental interactions in mammalian systems.

Shortest path analysis and ranking of cell cycle phase specific intermediates: We defined source-target relationships involved in regulation of each of the cell cycle phases as *viz.* $G1_{sources}$-$G1_{targets}$ as G1 phase regulators, $S_{sources}$-$S_{targets}$ as S phase regulators and $G1S_{sources}$-$G1S_{targets}$ as G1S phase regulators. We wished to identify key unique regulatory intermediates (IMP nodes) for a given source-target subset for regulating a particular phase of cell cycle. Shortest paths were calculated using Dijkstra's algorithm implemented in NetworkX. It takes approximately 1 hour to retrieve paths in a 2GB RAM workstation. . Shortest path lengths from source to target generally varied from 3 to 7, with several such paths often being present between a given source and target combination.

Algorithm: We defined the 2 path length PPI network to be our core network (N). Given a network N with a subset of nodes as sources (S) and targets (T) where S, T $\subset$ N we had to identify the intermediate nodes and quantify their occurrences for all pairs of S and T.

1. Trace all possible shortest paths between all pairs sources S and targets T.
2. Find the intermediate nodes (I) that occur in all possible shortest paths for a given S and T. Identify intermediate nodes I for all pairs of S and T.
3. Count the number of times each of the intermediate I occurs in shortest paths for all pairs of S and T.
4. Compute a z-score to normalize the occurrences of an intermediate with respect to the number of the source (S) and target (T) nodes for a given source-target subset.

$$IS_{S\text{-}T} = \frac{nI_{S\text{-}T} - \langle I_{S\text{-}T} \rangle}{\sigma I_{S\text{-}T}}$$

Where, $nI_{S\text{-}T}$ is the number of times the intermediate node I occurred in a given source- target subset, $\langle I_{S\text{-}T} \rangle$ is the median of number of occurrences of all intermediates nodes in the source-target subset, $\sigma I_{S\text{-}T}$ is the standard deviation of the number of occurrences of all intermediates nodes in the source-target subset.

5. This process of identifying the intermediates and scoring was repeated for all source-target subsets.
6. We employed a cut off criteria of intermediate score $IS_{S\text{-}T} \geq 1.28$ (p-value < 0.1) to shortlist only significantly high scoring intermediates for our further analysis.

Comparison and short listing of intermediates with control subsets.

Since we were interested in identifying the unique phase specific IMP nodes for G1, S and G1S phases of cell cycle we included a control criteria. Wherein molecules present in each

group was compared with the distinct source-target group (as shown in the table below). The overlapping or common molecules between these groups were filtered to retain only the unique nodes for each phase. Here, to facilitate comparison, a similar $G2_{source}$ to $G2_{target}$ analysis was also performed and the component nodes were similarly ranked. A cut-off Z-score of >1.28 (i.e. $p < 0.1$) was then employed for selecting the most frequently occurring nodes in all possible shortest paths for each of the cell cycle phases. From each of these individual lists, we next removed all those nodes that were also significantly present (i.e. Z-score > 1.28) in shortest paths describing the other, distinct, phases. That is, any intermediate short-listed in the $G1_{source}$ to $G1_{target}$ network was eliminated as a potential G1-specific IMP node if this node was also over-represented in shortest paths describing either the S, or the G2 phases. S-specific IMP nodes were delineated in a similar manner by comparing against the high-ranking node list from the G1 and G2 phases, whereas the G1S IMP nodes were identified by comparison against nodes from the G2 phase alone. We believe this analysis would further yield us highly phase specific IMP nodes for subsequent network analysis.

Phase specific regulatory source-target subset	Distinct control Networks
$G1_{sources}$-$G1_{targets}$	$S_{sources}$-$S_{targets}$ $G2_{sources}$-$G2_{targets}$
$S_{sources}$-$S_{targets}$	$G1_{sources}$-$G1_{targets}$ $G2_{sources}$-$G2_{targets}$
$G1S_{sources}$ -$G1S_{targets}$	$G2_{sources}$ -$G2_{targets}$

Intriguingly, with the exception of CDC25A, none of the source nodes described in Figure 2B were present in the list of extracted IMP nodes. This was in spite of the fact that shortest paths had been extracted from an undirected network thereby ensuring the absence of any inherent bias against their selection. A closer examination revealed that several of the nodes

from both groups were eliminated as possible IMP nodes because their frequency of occurrence was below the threshold value of significance. The remaining were then eliminated in the second round of selection since these nodes were also present as frequently occurring intermediates in the shortest paths describing the mutually exclusive cell cycle phases. Thus these nodes were either not enriched enough, or specific enough, to be extracted as cell cycle phase-specific IMP nodes.

***Extraction of phase specific IMP node subnetworks*:** We wanted to extract subnetwork regulating cell cycle phases incorporating the phase specific regulatory intermediates we identified earlier. We considered the phase specific intermediates as the seed list and traced all possible shortest paths of path length 2 between all pairs of nodes in the seed list. We identified the nodes present in the shortest paths of 2 path length between all pairs of seed nodes and merged them to create a connected subnetwork. This process was employed for all the three subsets of phase specific intermediates yielding three such networks of 2 path length.

***Identification of cell cycle phase specific regulatory motifs*:** Once we identified cell cycle phase specific subnetworks we wanted to resolve it further by manual literature curation on all the edges present in the subnetwork. By extensive manual literature curation we could include directions to the edges, for which the experimental evidence was present. We compiled a flat file with human Entrez gene name of source protein as the first column, target protein as the second column, '+' for activation interaction, '-' for inhibition and 0 for neutral interaction as the third. While the PMIDS for the interaction was a separate fourth column. This network was a mixed graph of both directed and undirected edges for each of the IMP node network (Table S7).

We used this network for identification of network motifs involving the phase specific IMP nodes. We used SNAVI [10], a software tool for network analysis, for motif detection in our literature curated IMP node subnetworks. With the phase specific regulatory intermediate nodes as seed list and the corresponding IMP node subnetwork as background we used SNAVI to identify the regulatory motifs for each phase separately. This yielded cell cycle phase specific motifs for G1, S and G1S phases, *viz.* scaffolds, bifans, feed-forward loops, feed-back loops (Figure 3D).

The number of scaffolds present in the G1S-specific IMP node network was 2-fold greater than that of G1-, and over 4-fold greater than that in the S phase-specific IMP node sub-network (Fig. 3D). Similarly, the numbers of Feed Forward Loops (FFLs), Bifans, and Diamond motifs were also significantly higher than the corresponding numbers present in either the G1 or the S phase sub-networks (Fig. 3D). The large number of FFLs identified in the G1S phase sub-network was particularly noteworthy. FFLs regulate both filtering of noise and signal amplification during signal transduction, and previous studies have suggested that they function as important transducers of signal to cell cycle responses [11]. Our findings may thus support that FFLs serve as the crucial signal-regulatory elements driving G1 to S phase transition. Further, the redundancy provided by over-representation of bifans and diamond motifs could contribute towards robustness of the system against external perturbations. Finally, our identification that the relative enrichment of signal-dependent regulatory motifs follows the order of G1S > G1 > S is consistent with fact that the G1/S checkpoint represents the step that is most tightly regulated by growth factor-mediated signaling [12,13].

Network Randomization of IMP nodes sub networks: In order to validate the motifs we identified in the phase specific IMP node networks to be functionally significant, we merged the IMP node networks (since there are overlapping interactions) to compile a single network

with mixed edges. This network was randomized over 100 times by shuffling the edge properties. Motifs involved by the phase specific IMP nodes were scanned for in the randomized networks using SNAVI. The figure 3E shows the results of the randomization exercise, thus statistically validating the motifs identified.

Computing Edge densities for the motif-clusters/Modules*:* To calculate the edge density of the modules, we took the IMP node network as the parent network and extracted 100 random sub-networks with the same number of nodes as were present in our motif cluster and calculated the edge-density for each of the random sub-networks. This was done for each of the cell cycle phases. As is typically done, edge-density was calculated by dividing the number of actual edges with the maximum number of possible edges. These values were then compared with that obtained for the motif clusters and the comparison is shown in the table below.

Cell Cycle Phase	Edge Density=2(E)/N(N-1)		
	Real motif cluster	Random subnetworks	Z-Score
G1 G1S S	0.08 0.05 0.38	0.03±0.01 0.02±0.006 0.10±0.05	4.16 4.47 5.66

Where E is the number of edges in the network and N is the number of nodes. It is evident from the above comparison that the edge-density of our motif clusters was at least 2.5-fold greater than the range of values obtained for the corresponding random sub-networks. That is, our motif clusters do exhibit at least some of the features that characterize network communities.

Cell cycle phase specific regulatory modules and regulators: We merged the motifs we identified for each phase to obtain a module for regulation of each phase. Since we wanted to

identify the least redundant nodes in the modules, we calculated centrality parameters *viz.* betweenness and stress. Stress centrality defines the ability of a node to hold together communicating nodes and, therefore, is representative of the degree of its involvement in regulatory processes [14]. Betweenness, on the other hand, is a more elaborate centrality index that describes the capacity of a node to serve as a junction in the network and, thereby, regulate the network in a coherent manner [14,15]. For this we employed a selection criteria where we shortlisted only those nodes exhibiting stress and betweenness greater then 2.5 times the mean of all nodes in the corresponding phases (Fig. 4A). This we consider would identify the statistically most important nodes for further examinations in the phase specific modules.

A detailed description of the pathway model shown in Figure 6.

We wanted to characterize the growth factor/mitogen activated signaling networks that drive the cell from the preparatory G1 phase, through the G1/S transition into the DNA synthetic phase. During the G1 phase the cell does the following,

1. It senses whether the extracellular conditions are permissive for cell growth and cell division.
2. If favourable conditions are present, it prepares to divide.

While it was initially thought that prolonged and continuous exposure to growth factors or mitogens was required to commit cells into the cycle, subsequent studies resolved that two short pulses of mitogen were sufficient to achieve this [16]. The initial pulse moved cells through the early stages of the G1 phase, while also making them responsive to the second pulse that followed several hours (~8h) later [16,17]. The second pulse then ensured progression through the later stages of G1, and consequent entry into the S phase [16]. These findings implicated the involvement of two discrete, and temporally segregated, signaling

cascades in the growth factor-dependent phase of the cell cycle. The precise nature of these signaling cascades and the manner in which they exert their regulatory effects remain incompletely characterized.

Given both the functional criteria employed to segregate the source nodes for our network analysis, and subsequent verification of the stage-specific relevance of the constituent vulnerable nodes, we reasoned that the G1- and G1S-IMP node modules extracted in Figure 4 in fact represented key modules that regulated the first and second 'wave' of mitogen-activated signals respectively. Consequently, the discerned distribution of the vulnerability indices of these molecules between the two modules was expected to yield insights into signaling mechanisms that regulated cell cycle commitment.

In the G1 IMP node network, AKT1 and PTK2B were the two kinases that were uniquely present as high-stress high-betweenness nodes, whereas SRC and the adaptor molecule GRB2 represented the least redundant constituents of both G1 and G1S modules (Fig. 4). That is, these four molecules likely represented key constituents of the signaling cascade that governs the early G1 phase of the cycle, with AKT1 and PTK2B playing a more specific role in this process. Of these, SRC is critical for the activation of AKT1, which in turn mediates the downstream processes required for cells to enter the cycle. Although several studies implicate a central role for AKT1 in the G1 phase [18], our present findings would however restrict its involvement to the early stages of this phase. Interestingly, examination of the known properties of these vulnerable nodes supports the inference that SRC serves as a common sensor that bridges AKT1 activation with both RTKs and mitogenic GPCRs. Whereas the SRC/GRB2 complex represents a constituent of the signalosome complex recruited by RTKs [19], both PTK2B and the membrane-associated pool of ESR1 (another vulnerable node in the G1 IMP node sub-network) mediate SRC activation by GPCRs [20]. This may then

explain earlier observations that distinct mitogenic signals activate a common signaling cascade in the early G1 response [21].

The nodes centred on the high stress betweeness nodes seem to work together to bring about the specific cellular outcomes. The nodes centred around the G1 high stress nodes such as AKT and PTK2B bring about the following specific functions-

1. Driving the cell towards survival by the inhibition of apoptotic signals/pathways.
2. Activation of Pro-survival and proliferative signals.
3. Promotion of protein synthesis.
4. Activation of pathways that increase transcription, activate, stabilize and phosphorylate cyclin D/CDK4 complexes which can phosphorylate Rb to initiate the cell cycle program.

The Receptor- SRC-AKT axis or early wave of signal may be required to initiate the cell cycle program by initiating the pro survival signals, promoting protein synthesis and activating survival signals. It involves the SRC dependent activation of the members of PI3K pathway, leading to the activation of AKT. Our G1 module therefore captures the critical molecules regulating key cellular processes which are needed to drive the cell through the early phase of G1.

It is evident from network of pathways shown in Figure 6 that this indeed represents an accurate synopsis of the multiplicity of biochemical events that cumulatively drive commitment of cells to the division cycle. More importantly it also reveals both the individual modes of functioning of the G1- and G1S-specific signaling cascades and the links between them that coordinate their respective activities. Thus, an examination of the relevant motifs in the merged module confirms that AKT1-dependent pathways indeed initiate cell

cycle progression, but in a manner that is supported by a concomitant inhibition of pro-apoptotic pathways, in addition to being coordinated with mechanisms regulating cell growth. For example, activation of cell cycle regulatory pathways by AKT1 was captured through its inhibitory effects on the CDK inhibitors p21 and p27, in addition to its positive effect on nuclear ESR1 that is mediated through inhibition of GSK3β. The active form of nuclear ESR1 then enhances *cyclin D1* transcription (Fig. 6). Further, there is also evidence to suggest that active AKT1 stabilizes the translated protein against proteosomal degradation [22]. The resulting increase in cyclin D1 levels, coupled with reduced CDK inhibitory activity, induces the formation of active cyclin D1/CDK complexes, thus marking initiation of the cell cycle. Here, concomitant activation of the transcription factor NFkB - mediated through AKT1-dependent phosphorylation of IKBKB - further adds by delivering a proliferative signal. Importantly, the activation of cell cycle regulatory mechanisms by AKT1 is also well complemented by its ability to simultaneously inhibit pro-apoptotic pathways of the cell. This is achieved through the inhibition of molecules such as BAD and caspases, as well as through inhibition of activation of members of the forkhead family of transcription factors (Fig. 6).

NFkB activation has also been implicated in regulation of cell growth by enhancing synthesis of specific proteins [23]. Our model indicates that this effect is further augmented through inhibition of the TSC complex by AKT1 (Fig. 6), which then activates mTOR a key regulator of protein synthesis and cell growth [22,23,24]. Thus, Figure 6 provides an integrated perspective on the central role played by AKT1 in driving cells through early G1. Presumably, this predominant reliance on a single signaling intermediate to regulate the complementary processes of cell cycle, cell growth, and promotion of cell survival, is critical for ensuring that they all function in concert with each other. Of particular note here is that the canonical MAP kinase pathway also supports the effector functions of AKT1 by

contributing towards these three processes [24,25]. Importantly, the SRC-mediated activation of this pathway - in a manner that is not strictly dependent upon either AKT1 or ABL1 – allows for its recruitment in both the early and late G1 (Fig. 6). Consequently, this pathway likely serves as at least one of the common links that facilitate transition between these two phases.

The G1S window is regulated through cooperative interactions between the cytoplasmic and nuclear pools of ABL1.

Figure 6 also rationalizes the key role ascribed to ABL1 during regulation of late G1 and the subsequent G1/S transition. While such an assignment is not inconsistent with the literature, our findings define the downstream mechanisms through which this kinase exerts its influence. Thus, activation of ERK5 by the cytoplasmic pool of ABL1 impacts on cell cycle progression via *c-fos* and cyclin D1 induction [26]. This effect is further reinforced through concomitant engagement of the JNK pathway. The resulting activation of JUN then promotes the synthesis of cyclins D and A, as well as that of the transcription factor MYC [27]. Facilitation of cell cycle progression by cytoplasmic ABL1 is well supported by its ability to also suppress the pro-apoptotic functions of p53. Further, a role during actin cytoskeleton reorganization is also captured in our model through the phosphorylation of WASL and related complexes (Fig. 6).

A prominent downstream consequence of cytoplasmic ABL1 activation is the enhancement in cellular c-MYC concentrations. At one level, this is achieved through the recruitment of a Ras-dependent pathway, which influences *MYC* transcription [28]. In addition, ABL1-induced activation of the JAK pathway also contributes significantly to this process. Activated JAKs are potent inducers of MYC since they function both by enhancing transcription, and by stabilizing the protein through inhibition of its proteasomal degradation

[28]. Thus, activation of cytoplasmic ABL1 translates into a multiplicity of mechanisms that collectively induce MYC upregulation. Here, the MAP kinase pathway also participates by phosphorylating MYC, and thereby protecting it against ubiquitinylation [28].

An important feature of our model is that it also highlights a role for the nuclear pool of ABL1 in regulating MYC levels. A significant proportion of nuclear ABL1 is normally maintained in an inactive form through its existence in a complex with RB [28]. As cells approach the G1/S boundary however, phosphorylation of RB causes the release of ABL1. At least some fraction of this released ABL1 interacts with JUN, as a result of which ABL is activated. This process then leads to the potent activation of JUN through a feedforward regulatory mechanism wherein ABL1 directly phosphorylates JUN, and also its upstream kinase JNK [28]. Thus, signaling pathways initiated from both the cytoplasmic and nuclear pools of ABL1 converge to activate JUN and, thereby, *MYC* upregulation. This cooperative action between the two ABL1 subsets may well explain the long-standing question of how cellular MYC levels are temporally modulated during cell cycle progression. While expression of this protein is induced in the early G1 phase these levels are, however, further enhanced as cells prepare for S phase entry [28]. This increase is likely essential for recruiting – through transcription regulatory mechanisms - the wider spectrum of biochemical activities that are required for driving G1 to S transition. Interestingly, consistent with our proposal, the timing of this second phase of MYC enhancement coincides with that of dissociation of the RB-ABL complex [28].

Downstream of ABL1, MYC functions as a central regulator that links external signals to the cell cycle machinery. In similarity with AKT1, it suppresses pro-apoptotic pathways while also facilitating cell growth through the activation of both ribosomal RNA and protein synthesis [29,30]. Importantly, the cell cycle-regulatory effects of MYC predominantly impinge on the later stages of G1, and thereby facilitate entry of cells into the S phase. These

include MYC-dependent transcription of E2Fs, positive regulation of cyclin E/CDK2 complexes, induction of Cdc25A, and the enhanced functional inactivation of CDK inhibitors [30]. Indeed the obligatory requirement for MYC during S phase entry is underscored by results demonstrating that either a reduction in its levels, or inhibition of its activity, causes a block in G1/S but not G0/G1 transition [30].

Thus the above analysis reiterates that our G1 and G1S IMP node modules indeed capture the core set of signaling processes that guide cells during the commitment phase of the cell cycle. Further, it also provides a mechanism-based rationalization of our earlier categorization - on the basis of graph theoretical considerations – of some of the nodes as displaying a high degree of vulnerability. Finally, this rationalization also extends to our assignment of key regulatory roles to AKT1 and ABL1 in the early and late G1 stages respectively.

Coordination of signal modulation with cell cycle progression.

A resolution to the issue of how ABL1 replaces AKT1 as the dominant signaling node in the G1S phase was also suggested from an analysis of the pathways captured by our model (Fig. 6). As illustrated, this process hinges upon the release of nuclear ABL1 from its complex with RB. AKTI-dependent initiation of cells into the cycle culminates with the phosphorylation of RB, which is normally evident by 8h after stimulation of cells with a mitogenic signal [17]. This leads to the release of bound ABL1. As noted earlier, activation of this subset synergizes with cytoplasmic ABL signaling to ensure enhancement in MYC levels. In addition, some fraction of this nuclear ABL1 is also likely to partition into the cytoplasmic compartment of the cell. This could be achieved either through its direct export in the non-phosphorylated form, or, following acetylation by the histone acetyltransferase

EP300 [31]. The resulting increase in the pool of cytoplasmic ABL1 would then further intensify signals generated from this subset of the kinase.

Thus, our model indicates a marked amplification of ABL1-dependent signaling as cells approach the G1/S boundary. This occurs through both enrichment of the cytoplasmic pool, as well as through activation of the fraction that remains in the nucleus. Importantly, this amplification would be further reinforced by the fact that signals from both subsets synergize at the level of activating downstream effector pathways such as MYC regulation, and the synthesis of cyclins. These cumulative effects may then explain how ABL1 acquires the characteristics of a vulnerable node in the later stages of G1. It is pertinent to recall here that although AKT1 is present in both the G1 and G1S modules, its properties of high-stress and high-betweenness are restricted to the G1 module (Fig. 4). That is, in the late G1 phase, ABL1 replaces AKT1 as the obligatory signaling intermediate. Significantly, this switch in signaling axes occurs in a seamless manner because, in addition to recruiting the additional pathways required for S phase entry, ABL1 also supplants the functions of AKT1 in terms of suppressing apoptotic pathways and regulating cell growth. This would then explain the increased functional redundancy of AKT1 at this stage.

Our proposal that signals from nuclear ABL1 contribute towards promoting cell cycle progression is apparently inconsistent with earlier findings that this subset primarily functions to activate the cellular apoptotic program in response to conditions such as genotoxic stress [32]. This latter activity, however, is strictly dependent upon its interactions with p53 and p73. As earlier discussed, mitogenic signals cause suppression of pro-apototic pathways, which include inhibition of activities of both p53 and p73. This is initiated in an AKT1-dependent manner in early G1, and then subsequently sustained by signals generated from cytoplasmic ABL1. We thus propose that activation of nuclear ABL1 under conditions where

pro-apoptotic pathways are inhibited biases its role towards integrating with the cell cycle stimulatory functions of its cytoplasmic counterpart.

REFERENCES.

1. Echeverri CJ, Perrimon N (2006) High-throughput RNAi screening in cultured cells: a user's guide. Nat Rev Genet 7: 373-384.
2. Neufeld TP, de la Cruz AF, Johnston LA, Edgar BA (1998) Coordination of growth and cell division in the Drosophila wing. Cell 93: 1183-1193.
3. Bader GD, Donaldson I, Wolting C, Ouellette BF, Pawson T, et al. (2001) BIND--The Biomolecular Interaction Network Database. Nucleic Acids Res 29: 242-245.
4. Stark C, Breitkreutz BJ, Reguly T, Boucher L, Breitkreutz A, et al. (2006) BioGRID: a general repository for interaction datasets. Nucleic Acids Res 34: D535-539.
5. Kerrien S, Alam-Faruque Y, Aranda B, Bancarz I, Bridge A, et al. (2007) IntAct--open source resource for molecular interaction data. Nucleic Acids Res 35: D561-565.
6. Chatr-aryamontri A, Ceol A, Palazzi LM, Nardelli G, Schneider MV, et al. (2007) MINT: the Molecular INTeraction database. Nucleic Acids Res 35: D572-574.
7. Keshava Prasad TS, Goel R, Kandasamy K, Keerthikumar S, Kumar S, et al. (2009) Human Protein Reference Database--2009 update. Nucleic Acids Res 37: D767-772.
8. Linding R, Jensen LJ, Pasculescu A, Olhovsky M, Colwill K, et al. (2008) NetworKIN: a resource for exploring cellular phosphorylation networks. Nucleic Acids Res 36: D695-699.
9. Matthews L, Gopinath G, Gillespie M, Caudy M, Croft D, et al. (2009) Reactome knowledgebase of human biological pathways and processes. Nucleic Acids Res 37: D619-622.
10. Ma'ayan A, Jenkins SL, Webb RL, Berger SI, Purushothaman SP, et al. (2009) SNAVI: Desktop application for analysis and visualization of large-scale signaling networks. BMC Syst Biol 3: 10.
11. Csikasz-Nagy A, Kapuy O, Toth A, Pal C, Jensen LJ, et al. (2009) Cell cycle regulation by feed-forward loops coupling transcription and phosphorylation. Mol Syst Biol 5: 236.
12. Sears RC, Nevins JR (2002) Signaling networks that link cell proliferation and cell fate. J Biol Chem 277: 11617-11620.
13. Zetterberg A, Larsson O, Wiman KG (1995) What is the restriction point? Curr Opin Cell Biol 7: 835-842.
14. Manimaran P, Hegde SR, Mande SC (2009) Prediction of conditional gene essentiality through graph theoretical analysis of genome-wide functional linkages. Mol Biosyst.
15. Newman MEJ (2005) A measure of betweenness centrality based on random walks. Social Networks 27: 39-54.
16. Jones SM, Kazlauskas A (2001) Growth-factor-dependent mitogenesis requires two distinct phases of signalling. Nat Cell Biol 3: 165-172.
17. Ezhevsky SA, Ho A, Becker-Hapak M, Davis PK, Dowdy SF (2001) Differential regulation of retinoblastoma tumor suppressor protein by G(1) cyclin-dependent kinase complexes in vivo. Mol Cell Biol 21: 4773-4784.
18. Massague J (2004) G1 cell-cycle control and cancer. Nature 432: 298-306.
19. Luttrell DK, Luttrell LM (2004) Not so strange bedfellows: G-protein-coupled receptors and Src family kinases. Oncogene 23: 7969-7978.
20. Litvak V, Tian D, Shaul YD, Lev S (2000) Targeting of PYK2 to focal adhesions as a cellular mechanism for convergence between integrins and G protein-coupled receptor signaling cascades. J Biol Chem 275: 32736-32746.
21. Jones SM, Kazlauskas A (2000) Connecting signaling and cell cycle progression in growth factor-stimulated cells. Oncogene 19: 5558-5567.

22. Gera JF, Mellinghoff IK, Shi Y, Rettig MB, Tran C, et al. (2004) AKT activity determines sensitivity to mammalian target of rapamycin (mTOR) inhibitors by regulating cyclin D1 and c-myc expression. J Biol Chem 279: 2737-2746.
23. Dan HC, Cooper MJ, Cogswell PC, Duncan JA, Ting JP, et al. (2008) Akt-dependent regulation of NF-{kappa}B is controlled by mTOR and Raptor in association with IKK. Genes Dev 22: 1490-1500.
24. Zhou BP, Liao Y, Xia W, Spohn B, Lee MH, et al. (2001) Cytoplasmic localization of p21Cip1/WAF1 by Akt-induced phosphorylation in HER-2/neu-overexpressing cells. Nat Cell Biol 3: 245-252.
25. Vincent AM, Feldman EL (2002) Control of cell survival by IGF signaling pathways. Growth Horm IGF Res 12: 193-197.
26. Brown JR, Nigh E, Lee RJ, Ye H, Thompson MA, et al. (1998) Fos family members induce cell cycle entry by activating cyclin D1. Mol Cell Biol 18: 5609-5619.
27. Obaya AJ, Mateyak MK, Sedivy JM (1999) Mysterious liaisons: the relationship between c-Myc and the cell cycle. Oncogene 18: 2934-2941.
28. Sirvent A, Benistant C, Roche S (2008) Cytoplasmic signalling by the c-Abl tyrosine kinase in normal and cancer cells. Biol Cell 100: 617-631.
29. Mateyak MK, Obaya AJ, Sedivy JM (1999) c-Myc regulates cyclin D-Cdk4 and -Cdk6 activity but affects cell cycle progression at multiple independent points. Mol Cell Biol 19: 4672-4683.
30. Amati B, Alevizopoulos K, Vlach J (1998) Myc and the cell cycle. Front Biosci 3: d250-268.
31. di Bari MG, Ciuffini L, Mingardi M, Testi R, Soddu S, et al. (2006) c-Abl acetylation by histone acetyltransferases regulates its nuclear-cytoplasmic localization. EMBO Rep 7: 727-733.
32. Dierov J, Dierova R, Carroll M (2004) BCR/ABL translocates to the nucleus and disrupts an ATR-dependent intra-S phase checkpoint. Cancer Cell 5: 275-285.